

ACKNOWLEDGMENTS

The author wishes to thank the committee for their time and help. In particular, the author wishes to thank Dr. Flaschka for his interest, support, and direction, and Dr. Kim for his encouragement and advice.

TABLE OF CONTENTS

LIST OF FIGURES	3
ABSTRACT	4
1. RAMANUJAN GRAPHS	5
1.1. Definitions	5
1.2. Families of Expanders and Ramanujan Graphs	6
2. CAYLEY GRAPHS	8
2.1. Constructing Cayley Graphs from Finite Abelian Groups	8
2.2. Constructing Quaternion Cayley Graphs	11
2.3. Properties of Quaternion Cayley Graphs	16
2.4. Proof that $X^{p,q}$ is connected	17
2.5. Bipartite $X^{p,q}$	20
3. RANDOM GRAPHS	21
3.1. Construction of Random, Simple, 7-Regular Graphs	21
3.2. Distribution of Eigenvalues	24
3.3. Distribution of Eigenvalue Spacings	24
3.4. Random, 7-regular, Ramanujan Graphs	27
3.5. Edge Behavior	28
3.6. Scaling Parameters and Distributions of S_1 and S_{n-1}	30
3.7. Inconsistencies	34
4. AREAS FOR FUTURE WORK	36
5. APPENDIX 1: REPRESENTATIVES OF $PGL_2(5)$	38
REFERENCES	40

LIST OF FIGURES

FIGURE 2.1. The Cayley Difference Graph $X(G, S)$ for $G = \mathbf{Z}/5\mathbf{Z}$ and $S =$ the set of squares	11
FIGURE 3.1. Cycle and Toothpick Graphs on 6 vertices	22
FIGURE 3.2. Permuted Cycle and Toothpick Graphs on 6 Vertices	23
FIGURE 3.3. Resulting 7 Regular Graph	23
FIGURE 3.4. Eigenvalue Distribution for Simple, 7-Regular Graphs vs. the McKay density $f_k(x)$	25
FIGURE 3.5. $\left(\frac{k(k-1)}{k^2-4(k-1)y^2}\right)$ plotted over the support of $\tilde{f}_k(y)$ for various k	26
FIGURE 3.6. Distribution of scaled eigenvalue spacings for our simple 7-regular graphs vs. the Wigner surmise	27
FIGURE 3.7. Log Log plot of $\langle \lambda_1 - 2\sqrt{6} \rangle$ and $ \langle -\lambda_{n-1} - 2\sqrt{6} \rangle $ vs. matrix size n , as n ranges over the sizes 100, 200, 400, 500, 600, 800, 1000, 1500, and 2000 corresponding to samples of 1000, 1000, 1000, 1504, 1000, 1500, 1265, 7347, and 1000 matrices respectively.	30
FIGURE 3.8. Plot of the Tracy-Widom distributions f_1 and f_4	31
FIGURE 3.9. Empirical cumulative density function of S_1 plotted against the Tracy-Widom c.d.f., F_4 , for various values of n . F_4 is shifted by 2 to the right, and the scaling parameters are $\beta_1 = \frac{3}{5}$ and $C_1 = \frac{3}{4}$	32
FIGURE 3.10. Empirical cumulative density function of S_{n-1} plotted against the Tracy-Widom c.d.f., F_1 , for various values of n . F_1 is shifted by $\frac{1}{8}$ to the right, and the scaling parameters are $\beta_{n-1} = \frac{5}{8}$ and $C_{n-1} = \frac{4}{5}$	33

ABSTRACT

Coalescing algebraic geometry, representation theory, number theory, and random matrix theory, Ramanujan graphs are of great interest both in pure and applied mathematics. This paper discusses various constructions of Ramanujan graphs, and the spectra of their adjacency matrices. In section one, the relevant terminology is given, properties of graphs are explored, and Ramanujan graphs are defined. In section two, explicit constructions of Ramanujan Cayley graphs are explored and properties of these graphs are discussed. In section three, results of numerical experiments generating random 7-regular graphs are presented, the spectra of these random graphs are examined, and similarities with established distributions are investigated. Areas for future research are presented in section four. Sections two and three can be read independently.

1. RAMANUJAN GRAPHS

In this section we present some of the basic terminology of graph theory and explore some of the fundamental properties of graphs. In particular, we examine bounds on the isoperimetric constant and define Ramanujan graphs.

1.1. Definitions

A graph X is composed of a set of vertices, $V(X)$, and a set of edges, $E(X)$, whose endpoints are elements of $V(X)$. If an edge connects a vertex to itself, it is called a *loop*. There may be multiple edges in the set $E(X)$ connecting the same vertices in $V(X)$. If a graph has no loops or multiple edges it is called *simple*, otherwise it is called a *multigraph*. Two vertices are said to be *adjacent* if there is an edge connecting them. A graph is *bipartite* if $V(X)$ can be partitioned into two sets, V_- and V_+ such that no two vertices of V_- , or V_+ , are adjacent. A graph is said to be *connected* if for any pair of vertices v_i, v_j in $V(X)$, there exists a sequence $v_i, v_1, v_2, \dots, v_m, v_j$ such that all vertices in the sequence are elements of $V(X)$ and any two consecutive vertices are adjacent. The number of edges emanating from a given vertex is known as the vertex degree. Loops are counted as two edges emanating from the vertex. If every vertex in the graph has degree k , the graph is called *k -regular*. The *girth* of a graph X , denoted $g(X)$, is the length of the shortest circuit, (i.e. the shortest closed path in X).

Every graph can be described by an *adjacency matrix*, denoted $A(X)$. If X is a graph with n vertices, the adjacency matrix is the $n \times n$ matrix defined by:

$$(A(X))_{i,j} = \text{the number of edges between vertex } v_i \text{ and vertex } v_j \quad (1.1)$$

Since the edges in $E(X)$ are undirected¹, if v_i is adjacent to v_j , v_j must be adjacent to v_i . Thus, $(A(X))_{i,j} = (A(X))_{j,i}$. The spectrum of the graph X is the spectrum of the associated adjacency matrix, $A(X)$. Since $A(X)$ is symmetric, the spectrum of X is real.

Theorem 1. *If X is a k -regular graph on n vertices, the spectrum of X takes the form*

$$k = \mu_0 \geq \mu_1 \geq \mu_2 \geq \dots \geq \mu_{n-1} \quad (1.2)$$

where $\mu_{n-1} \geq -k$, and the multiplicity of k is equal to the number of connected components of X . The smallest eigenvalue μ_{n-1} , is equal to $-k$ if and only if X is bipartite. The eigenvalues in the spectrum of X equal to $\pm k$ are called the trivial eigenvalues.

¹If the edges are directed, the graph is called a digraph

1.2. Families of Expanders and Ramanujan Graphs

For any subset $F \subseteq V(X)$, the *boundary*, ∂F , of F is defined as the set of edges $\{e = xy \mid x \in F \text{ and } y \in V - F\} \subseteq E(X)$.

Definition. The *expanding*, or *isoperimetric*, constant, $h(X)$ is defined as

$$h(X) = \inf \left\{ \frac{|\partial F|}{\min\{|F|, |V - F|\}} \quad : \quad 0 < |F| \leq |V| \right\} \quad (1.3)$$

Thus, the expanding constant gives a lower bound on how well any subset of the vertices is connected to the rest of the vertices in the graph. If $h(X)$ is small, there exists a subset $F_0 \subseteq V(X)$ such that F_0 is connected to the rest of the vertices of X by only a few edges. If the graph is disconnected, $h(X) = 0$. Larger $h(X)$ correspond to better expander graphs X .

Definition. If (X_m) is a family of finite², connected, k -regular graphs, with the index $m \geq 1$, and $|V(X_m)| \rightarrow \infty$ as $m \rightarrow \infty$, then (X_m) is a *family of expanders* if there exists an $\epsilon > 0$ such that $h(X) \geq \epsilon$ for all $m \geq 1$.

Theorem 2. *For any finite, connected, k -regular graph, X , without loops, the expanding constant is bounded by*

$$\frac{k - \mu_1}{2} \leq h(X) \leq \sqrt{2k(k - \mu_1)} \quad (1.4)$$

Thus, the greater the spectral gap, $k - \mu_1$, the better the expander. From Theorem 2, we see that if $\mu_1(X_m)$ is the second largest eigenvalue in the spectrum of X_m , (X_m) is a family of expanders if and only if there exists an $\epsilon > 0$ such that $k - \mu_1(X_m) \geq 2\epsilon$ for all $m \geq 1$. The following theorem provides an upper bound on the spectral gap in the limit as $m \rightarrow \infty$.

Theorem 3.

$$\liminf_{m \rightarrow \infty} \mu_1(X_m) \geq 2\sqrt{k - 1} \quad (1.5)$$

From a spectral point of view, an optimal family of expanders is one for which $\mu_1(X_m) = 2\sqrt{k - 1}$ in the limit as $m \rightarrow \infty$. This leads to the idea of Ramanujan graphs.

Definition. A finite, connected, k -regular graph, X , is *Ramanujan* if and only if

$$|\mu_i| \leq 2\sqrt{k - 1} \quad (1.6)$$

for all non-trivial eigenvalues μ_i of X .

²A graph is finite if $|V(X)| < \infty$

Thus, a family of Ramanujan graphs achieves the greatest possible spectral gap in the limit as $m \rightarrow \infty$. Methods of constructing k -regular Ramanujan graphs are discussed in the next section. These methods only generate families of Ramanujan graphs for particular values of k . The first value of k for which there is no known explicit construction is $k = 7$. In section 3 we examine randomly generated, 7-regular graphs, and determine which of these random graphs are Ramanujan.

2. CAYLEY GRAPHS

Cayley graphs are a special class of k -regular graphs constructed using group theory. Since these graphs are built up from a particular group G , we can use this underlying group, or its irreducible representations, to analyze the spectrum of the graph. In particular, we can determine whether a particular Cayley graph is Ramanujan without constructing its adjacency matrix. Since calculating the spectrum of an $N \times N$ matrix is computationally expensive for large N , the ability to determine whether a given graph is Ramanujan without constructing its adjacency matrix is very useful. In this section we examine Cayley graph constructions based on finite abelian groups, and quaternion algebras, and describe when these constructions result in Ramanujan graphs.

Definition. Given a finite group G , a k -element multiset of G is a subset S consisting of k elements, allowing repetitions. If for all s in S , $s^{-1} \in S$, we say S is *symmetric*.

Definition. Given a finite group G and a k -element symmetric multiset S , the Cayley Difference Graph $X(G, S)$ is the graph defined by $V(X) = G$, and $E(X) = \{e = xy \mid x^{-1}y = s \in S\}$.

The number of edges between vertex x and vertex y is equal to the multiplicity of the element $s = x^{-1}y$ in S . Since S has k elements, the resulting graph is k -regular. This definition can be generalized to non-symmetric, k -element multisets S , in which case the resulting graph is a k -regular digraph. The Cayley difference graph $X(G, S)$ is connected if and only if the set S generates the group G .

2.1. Constructing Cayley Graphs from Finite Abelian Groups

The following theorem allows us to determine *a priori* whether a given finite abelian group G , with symmetric, k -element multiset S , will produce a Ramanujan graph under the Cayley construction.

Theorem 4. *If G is a finite abelian group and S is a symmetric, k -element multiset, then the eigenvalues of the adjacency matrix $A(X(G, S))$ are given by*

$$\lambda_\chi = \sum_{s \in S} \chi(s) \tag{2.1}$$

as χ ranges over the irreducible characters of G . [4]

Proof. For each irreducible character χ , let $(\vec{v}_\chi)_i = \chi(g_i)$ where g_i is the i^{th} element of G . Thus, if $|G| = n$, \vec{v}_χ is the n -dimensional vector of the character χ evaluated at the n elements of G . Define δ_S as follows:

$$\delta_S(s) = \begin{cases} 0 & \text{if } s \notin S \\ m & \text{if } s \in S \text{ with multiplicity } m \end{cases}$$

We note that,

$$\begin{aligned} (A(X(G, S)))_{ij} &= \text{the number of edges between vertex } g_i \text{ and vertex } g_j \\ &= \text{the multiplicity of } g_i^{-1}g_j \text{ in } S \\ &= \delta_S(g_i^{-1}g_j) \end{aligned}$$

$$\begin{aligned} \text{Thus } (A(X) \cdot \vec{v}_\chi)_i &= \sum_{j=1}^n a_{ij} \cdot \chi(g_j) \\ &= \sum_{g_j \in S} \delta_S(g_i^{-1}g_j) \cdot \chi(g_j) \quad \text{let } x_g = g_i^{-1}g_j \Rightarrow \\ (A(X) \cdot \vec{v}_\chi)_i &= \sum_{g_i \in S} \delta_S(x_g) \cdot \chi(g_i \cdot x_g) \\ &= \sum_{s \in S} \chi(g_i \cdot s) \\ &= \sum_{s \in S} \chi(g_i) \cdot \chi(s) \quad \text{Since all irreducible representations} \\ & \hspace{15em} \text{of } G \text{ are 1-dimensional} \\ &= \chi(g_i) \sum_{s \in S} \chi(s) \end{aligned}$$

Thus \vec{v}_χ is an eigenvector of the adjacency matrix $A(X(G, S))$, with associated eigenvalue $\sum_{s \in S} \chi(s)$. Furthermore, since G is abelian, the number of distinct conjugacy classes is equal to $|G|$. Thus, by the Group Orthogonality Theorem, the number of irreducible representations of $G = n$. Therefore, equation 2.1 generates all n eigenvalues of $A(X(G, S))$ as χ varies over the irreducible characters of G . \square

Observation 1. For any abelian group G , the *irreducible trivial character*

$$\chi_T(g) = 1 \quad \forall g \in G.$$

Since $S \subset G$ and $|S| = k$, the sum $\sum_{s \in S} \chi_T(s) = k$. It follows that $X(G, S)$ is Ramanujan if and only if

$$1. \lambda_\chi \neq k \quad \forall \chi \neq \chi_T$$

2. $|\lambda_\chi| = |\sum_{s \in S} \chi(s)| \leq 2\sqrt{k-1}$ for any non-trivial eigenvalue of $X(G, S)$.

Criterion 1 is the same as requiring that X be connected, or equivalently, that S generate G .

The following example illustrates the process of constructing a Ramanujan graph from a finite abelian group G .

Example. Let $G = \mathbf{Z}/5\mathbf{Z}$ and take S to be the set of squares, with 0 included twice ¹. Thus, $S = \{0^2, 0^2, 1^2, 2^2, 3^2, 4^2\} = \{0, 0, 1, 4, 4, 1\}$. Since 1 and 4 are additive inverses in $\mathbf{Z}/5\mathbf{Z}$, S is a symmetric, 6-element multiset. Let χ be any irreducible character of G . Since $\mathbf{Z}/5\mathbf{Z}$ is a cyclic group of order 5, it follows that $\chi(g)^5 = \chi(g+g+g+g+g) = \chi(e) = 1 \quad \forall g \in G$. Thus, for all g in G and for any irreducible character χ , $\chi(g)$ must be a 5th root of unity. Thus, the irreducible characters of $G = \mathbf{Z}/5\mathbf{Z}$ are:

$$\begin{array}{l} \chi_T : \chi_T(g) = 1 \quad \forall g \in G \\ \chi_2 : \chi_2(0) = 1 \quad \chi_2(1) = e^{2\pi i/5} \quad \chi_2(2) = e^{4\pi i/5} \quad \chi_2(3) = e^{6\pi i/5} \quad \chi_2(4) = e^{8\pi i/5} \\ \chi_3 : \chi_3(0) = 1 \quad \chi_3(1) = e^{4\pi i/5} \quad \chi_3(2) = e^{8\pi i/5} \quad \chi_3(3) = e^{2\pi i/5} \quad \chi_3(4) = e^{6\pi i/5} \\ \chi_4 : \chi_4(0) = 1 \quad \chi_4(1) = e^{6\pi i/5} \quad \chi_4(2) = e^{2\pi i/5} \quad \chi_4(3) = e^{8\pi i/5} \quad \chi_4(4) = e^{4\pi i/5} \\ \chi_5 : \chi_5(0) = 1 \quad \chi_5(1) = e^{8\pi i/5} \quad \chi_5(2) = e^{6\pi i/5} \quad \chi_5(3) = e^{4\pi i/5} \quad \chi_5(4) = e^{2\pi i/5} \end{array}$$

According to equation 2.1, the eigenvalues of $A(X(G, S))$ are given by:

$$\begin{aligned} \lambda_{\chi_T} &= \sum_{s \in S} \chi_T(s) = 2\chi_{ITR}(0) + 2\chi_{ITR}(1) + 2\chi_{ITR}(4) = 2 + 2 + 2 = 6 \\ \lambda_{\chi_2} &= \sum_{s \in S} \chi_2(s) = 2 + 2e^{2\pi i/5} + 2e^{8\pi i/5} = 3.236 \dots \\ \lambda_{\chi_3} &= \sum_{s \in S} \chi_3(s) = 2 + 2e^{4\pi i/5} + 2e^{6\pi i/5} = -1.236 \dots \\ \lambda_{\chi_4} &= \sum_{s \in S} \chi_4(s) = 2 + 2e^{4\pi i/5} + 2e^{6\pi i/5} = -1.236 \dots \\ \lambda_{\chi_5} &= \sum_{s \in S} \chi_5(s) = 2 + 2e^{2\pi i/5} + 2e^{8\pi i/5} = 3.236 \dots \end{aligned}$$

From the previous calculation we see that $|\lambda_{\chi_i}| \leq 2\sqrt{6-1}$ for all irreducible characters $\chi_i \neq \chi_T$. Thus, $X(G, S)$ is a 6-regular Ramanujan multigraph.

Carrying out the construction of the Cayley graph $X(G, S)$, we find that $X(G, S)$ is a 6-regular graph with adjacency matrix:

$$A(X(G, S)) = \begin{bmatrix} 2 & 2 & 0 & 0 & 2 \\ 2 & 2 & 2 & 0 & 0 \\ 0 & 2 & 2 & 2 & 0 \\ 0 & 0 & 2 & 2 & 2 \\ 2 & 0 & 0 & 2 & 2 \end{bmatrix}$$

¹By including 0 twice, S is a symmetric multiset

having eigenvalues $\{6, 3.236\dots, 3.236\dots, -1.236\dots, -1.236\dots\}$.

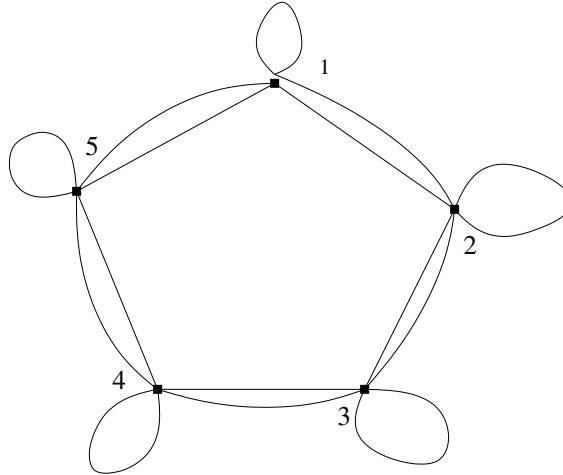


FIGURE 2.1. The Cayley Difference Graph $X(G, S)$ for $G = \mathbf{Z}/5\mathbf{Z}$ and $S =$ the set of squares

While Cayley graphs constructed from finite abelian groups are pleasing aesthetically and provide a straightforward example of the Cayley construction method, since S is often a multiset in this construction, the resulting graph is often a multigraph. A more useful Cayley graph construction based on quaternion algebras is laid out in [1] and described below.

2.2. Constructing Quaternion Cayley Graphs

The quaternion Cayley graph construction can generate infinitely many k -regular graphs for any $k = p + 1$, where p is an odd prime. Furthermore, the resulting graphs are simple.

The following definitions are necessary in describing the quaternion Cayley graph construction.

Definition. For an odd prime p , let Λ' be the subset of the integral quaternions,

$$\Lambda' = \left\{ \alpha \in \mathbf{H}(\mathbf{Z}) \mid \begin{array}{l} \alpha \equiv 1 \pmod{2} \text{ or } \alpha \equiv i + j + k \pmod{2}, \\ \text{and } N(\alpha) = p^m \text{ for some value } m \end{array} \right\} \quad (2.2)$$

where $N(\alpha)$ is the norm of $\alpha = a_0 + a_1i + a_2j + a_3k$, defined by $N(\alpha) = a_0^2 + a_1^2 + a_2^2 + a_3^2$.

There are $8(p + 1)$ solutions to the equation

$$N(\alpha) = a_0^2 + a_1^2 + a_2^2 + a_3^2 = p. \quad (2.3)$$

If α is a solution, then so too are the 8 associates² $\varepsilon\alpha$, of α . Thus, up to associates, there are $p + 1$ solutions of $N(\alpha) = p$. If $p \equiv 1 \pmod{4}$ then one of the a_i is odd and the rest are even. If $p \equiv 3 \pmod{4}$ then one of the a_i is even and the rest are odd. In either case, for each solution α , one a_i is distinguished from the rest. Among the 8 associates of a particular solution α , if $a_i \neq 0$, only one will have $a_0 = |a_i|$. Let S_p denote the set of these distinguished solutions. If $a_i = 0$, select only one of the two associates with $a_0 = 0$ to be an element of S_p . Thus, $|S_p| = p + 1$. Requiring a_0 to be the distinguished component implies $S_p \subset \Lambda'$.

Definition.

$$S_p = \left\{ \alpha \in \Lambda' \mid \begin{array}{l} N(\alpha) = p, a_0 \geq 0 \\ \text{and, if } a_0 = 0, -\alpha \notin S_p \end{array} \right\} \quad (2.4)$$

Let τ_q be reduction mod q . Thus, $\tau_q : \Lambda' \rightarrow \mathbf{H}(\mathbf{F}_q)^\times$. If q is sufficiently large³, $\tau_q(S_p) = S_p$.

Let $\psi_q : \mathbf{H}(\mathbf{F}_q)^\times \rightarrow \mathbf{GL}_2(\mathbf{q})$ be the isomorphism defined by

$$\psi_q(a_0 + a_1i + a_2j + a_3k) = \begin{bmatrix} a_0 + a_1x + a_3y & -a_1y + a_2 + a_3x \\ -a_1y - a_2 + a_3x & a_0 - a_1x - a_3y \end{bmatrix} \quad (2.5)$$

where $x, y \in \mathbf{F}_q$ such that $x^2 + y^2 + 1 \equiv 0 \pmod{q}$.

Let ϕ be the homomorphism defined by

$$\phi \left(A = \begin{bmatrix} a & b \\ c & d \end{bmatrix} \right) = \phi_A(z) = \frac{az + b}{cz + d} \quad (2.6)$$

and let $S_{p,q} = \phi \circ \psi_q \circ \tau_q(S_p)$.

Given the previous definitions and the observation that $\phi(GL_2(q)) \cong PGL_2(q)$, we have the following diagram.

$$\begin{array}{ccccc} S_p \subset \Lambda' & \xrightarrow{\tau_q} & \mathbf{H}(\mathbf{F}_q)^\times & \xrightarrow{\psi_q} & GL_2(q) \\ & & & & \downarrow \phi \\ & & & & S_{p,q} \subseteq PGL_2(q) \end{array} \quad (2.7)$$

Claim 1. $S_{p,q}$ is a symmetric subset of $PGL_2(q)$ when ⁴ $\left(\frac{p}{q}\right) = -1$, and $PSL_2(q)$

² $\varepsilon\alpha$ is an associate of α if and only if ε is a unit, i.e. $\varepsilon \in \{\pm 1, \pm i, \pm j, \pm k\}$.

³ $q > 2\sqrt{p}$ will suffice

⁴ $\left(\frac{p}{q}\right)$ is the Legendre symbol.

$$\left(\frac{p}{q}\right) = \begin{cases} 0 & \text{if } q|p \\ 1 & \text{if } q \nmid p \text{ and } p = b^2 \pmod{q} \\ -1 & \text{if } q \nmid p \text{ and } \nexists b \in \mathbf{Z}_q \ni p = b^2 \pmod{q} \end{cases}$$

when $\left(\frac{p}{q}\right) = 1$.

Proof. From the definition of S_p (2.4), if $\alpha = a_0 + a_1i + a_2j + a_3k \in S_p$ and $a_0 > 0$, then $\bar{\alpha}$ is also an element of S_p . Furthermore, if $\beta = b_0 + b_1i + b_2j + b_3k \in S_p$ and $b_0 = 0$, then $\bar{\beta} = -\beta$ is not an element of S_p . Thus, S_p has the form

$$S_p = \{\alpha_1, \bar{\alpha}_1, \alpha_2, \bar{\alpha}_2, \dots, \alpha_s, \bar{\alpha}_s, \beta_1, \beta_2, \dots, \beta_t\}$$

where $2s + t = p + 1$.

For all $\alpha \in S_p$ such that $a_0 > 0$, $\varphi \circ \psi_q \circ \tau_q(\alpha)$ and $\varphi \circ \psi_q \circ \tau_q(\bar{\alpha})$ are elements of $S_{p,q}$. Furthermore,

$$[\varphi \circ \psi_q \circ \tau_q(\alpha)] \cdot [\varphi \circ \psi_q \circ \tau_q(\bar{\alpha})] = \varphi \circ \psi_q \circ \tau_q(\alpha \cdot \bar{\alpha}) \quad (2.8)$$

Two facts follow directly from the definition of ψ_q (2.5),

1. $\det(\psi_q(\alpha)) = N(\alpha) \pmod{q}$
2. $\forall \alpha_q \in \mathbf{H}(\mathbf{F}_q)$ such that $\alpha_q = \bar{\alpha}_q$ (i.e. for all “real” $\alpha_q \in \mathbf{H}(\mathbf{F}_q)$), $\psi_q(\alpha_q)$ is a scalar matrix⁵

Since $\alpha \cdot \bar{\alpha} = \bar{\alpha} \cdot \alpha = \overline{\alpha \cdot \bar{\alpha}}$, it follows that $\tau_q(\alpha \cdot \bar{\alpha}) = \overline{\tau_q(\alpha \cdot \bar{\alpha})}$. Thus, $\psi_q(\tau_q(\alpha \cdot \bar{\alpha}))$ is a scalar matrix, which implies $\psi_q(\tau_q(\alpha \cdot \bar{\alpha})) \in \ker(\varphi)$. Therefore, by equation 2.8, $[\varphi \circ \psi_q \circ \tau_q(\alpha)]^{-1} = [\varphi \circ \psi_q \circ \tau_q(\bar{\alpha})]$.

If $\beta \in S_p$ such that $b_0 = 0$ then $\bar{\beta} \notin S_p$, however

$$\begin{aligned} [\varphi \circ \psi_q \circ \tau_q(\beta)] \cdot [\varphi \circ \psi_q \circ \tau_q(\bar{\beta})] &= \varphi \circ \psi_q \circ \tau_q(\beta \cdot \bar{\beta}) \\ &= \varphi \circ \psi_q \circ \tau_q(-\beta\bar{\beta}) \\ &= \varphi(-\psi_q(\tau_q(\beta\bar{\beta}))) \\ &= \varphi\left(-\begin{pmatrix} \lambda & 0 \\ 0 & \lambda \end{pmatrix}\right) = 1 \end{aligned}$$

Thus, $[\varphi \circ \psi_q \circ \tau_q(\beta)]^{-1} = [\varphi \circ \psi_q \circ \tau_q(\bar{\beta})]$.

Therefore, for all $[\varphi \circ \psi_q \circ \tau_q(s)]$ in $S_{p,q}$, $[\varphi \circ \psi_q \circ \tau_q(s)]^{-1}$ is also in $S_{p,q}$. $S_{p,q}$ is a symmetric subset of $PGL_2(q)$.

Lemma 1. *If $\left(\frac{p}{q}\right) = 1$ then $S_{p,q} \subset PSL_2(q)$.*

⁵That is to say $\psi_q(\alpha_q) = \begin{pmatrix} \lambda & 0 \\ 0 & \lambda \end{pmatrix}$ for some $\lambda \in \mathbf{Z}_q$.

Proof. For all α in S_p , $N(\alpha) = p$. By (2.5), $\det(\psi_q(\tau_q(\alpha))) = N(\alpha) \pmod q$. Thus, if $\left(\frac{p}{q}\right) = 1$, $\psi_q \circ \tau_q(\alpha)$ is equal to some 2×2 matrix with determinant $p = b^2 \pmod q$ for some $b \in \mathbf{Z}_q$. Let

$$\begin{aligned} \psi_q \circ \tau_q(\alpha) = A &= \begin{bmatrix} a & b \\ c & d \end{bmatrix} \\ A &\sim \begin{bmatrix} b^{-1} & 0 \\ 0 & b^{-1} \end{bmatrix} A \quad \text{in } PGL_2(q) \end{aligned}$$

Thus,

$$[A] = \left[\begin{pmatrix} b^{-1} & 0 \\ 0 & b^{-1} \end{pmatrix} A \right] \in PGL_2(q). \quad (2.9)$$

But,

$$\begin{aligned} \det \left(\begin{bmatrix} b^{-1} & 0 \\ 0 & b^{-1} \end{bmatrix} A \right) &= \det \left(\begin{bmatrix} b^{-1} & 0 \\ 0 & b^{-1} \end{bmatrix} \right) \det(A) \\ &= 1, \end{aligned} \quad (2.10)$$

which implies, $[A] \in PSL_2(q)$.

Thus, for every $\alpha \in S_p$, if $\left(\frac{p}{q}\right) = 1$, $\varphi \circ \psi_q \circ \tau_q(\alpha)$ is an element of $PSL_2(q)$. Hence, $S_{p,q} = \varphi \circ \psi_q \circ \tau_q(S_p) \subset PSL_2(q)$.

Furthermore, if $\left(\frac{p}{q}\right) = -1$ then there is no $b \in \mathbf{Z}_q$ such that $p \equiv b^2 \pmod q$, which implies there is no $\begin{pmatrix} \lambda & 0 \\ 0 & \lambda \end{pmatrix} \in GL_2(q)$ such that $\det \left[\begin{pmatrix} \lambda & 0 \\ 0 & \lambda \end{pmatrix} \cdot (\psi_q \circ \tau_q(\alpha)) \right] = 1$ □

Thus, if $\left(\frac{p}{q}\right) = -1$, then for all $\alpha \in S_p$, $\psi_q \circ \tau_q(\alpha) = A$ is not congruent to any matrix with $\det = 1$ in $PGL_2(q)$. In other words, $[A] \in PGL_2(q) - PSL_2(q)$. Thus, if $\left(\frac{p}{q}\right) = -1$, it follows that

$$S_{p,q} \subset PGL_2(q) - PSL_2(q). \quad (2.11)$$

□

Now that we have established a $p + 1$ element, symmetric subset of $PGL_2(q)$ when $\left(\frac{p}{q}\right) = -1$, and of $PSL_2(q)$ when $\left(\frac{p}{q}\right) = 1$, we can define the Quaternion Cayley Graph.

Definition. Given odd primes p and q , the Quaternion Cayley Graph $X^{p,q}$ is the Cayley Difference graph $X(G, S_{p,q})$ where

$$G = \begin{cases} PGL_2(q) & \text{when } \left(\frac{p}{q}\right) = -1 \\ PSL_2(q) & \text{when } \left(\frac{p}{q}\right) = 1 \end{cases}$$

Example. To illustrate the quaternion Cayley construction, consider the simplest possible example. Let $p = 3$ and $q = 5$. Since $\left(\frac{3}{5}\right) = -1$, $X^{p,q} = X(PGL_2(5), S_{3,5})$. By definition, $PGL_2(5) = GL_2(5) / \left\{ \begin{pmatrix} \lambda & 0 \\ 0 & \lambda \end{pmatrix} : \lambda \in \mathbf{Z}_5^\times \right\}$. Using a purely combinatorial argument we find $|PGL_2(q)| = q(q^2 - 1)$. Thus, $|PGL_2(5)| = 120$. We can represent all equivalence classes of $PGL_2(5)$ with the matrices listed in appendix 1. For $p = 3$, $q = 5$, S_p equals the distinguished set of integral solutions of $a_0^2 + a_1^2 + a_2^2 + a_3^2 = 3$, namely

$$S_p = \{s_1 = i + j + k, \quad s_2 = -i + j + k, \quad s_3 = i - j + k, \quad s_4 = i + j - k\} \quad (2.12)$$

Thus $\tau_q(S_p) = S_p$. Using $x = 2$ and $y = 0$ in the definition of ψ_q , we find

$$\phi(\psi_q(S_p)) = \left\{ \begin{bmatrix} 2 & 3 \\ 1 & -2 \end{bmatrix}, \quad \begin{bmatrix} -2 & 3 \\ 1 & 2 \end{bmatrix}, \quad \begin{bmatrix} 2 & 1 \\ 3 & -2 \end{bmatrix}, \quad \begin{bmatrix} 2 & -1 \\ -3 & -2 \end{bmatrix} \right\} \subset PGL_2(5), \quad (2.13)$$

or equivalently

$$\phi(\psi_q(S_p)) = \left\{ \begin{bmatrix} 1 & 4 \\ 3 & 4 \end{bmatrix}, \quad \begin{bmatrix} 1 & 1 \\ 2 & 4 \end{bmatrix}, \quad \begin{bmatrix} 1 & 3 \\ 4 & 4 \end{bmatrix}, \quad \begin{bmatrix} 1 & 2 \\ 1 & 4 \end{bmatrix} \right\} \subset PGL_2(5), \quad (2.14)$$

By definition of the Cayley difference graph,

$$(A(X^{p,q}))_{i,j} = (A(X(PGL_2(q), S_{p,q})))_{i,j} \neq 0 \quad \text{if and only if} \quad [A_j] = [A_i] \cdot [s]$$

for some $[s] \in \phi(\psi_q(\tau_q(S_p)))$. For example, the vertex $[A_2] = \begin{bmatrix} 1 & 0 \\ 0 & 2 \end{bmatrix}$ is adjacent to the vertices $\{[A_{60}], [A_{75}], [A_{98}], [A_{111}]\}$, since $[A_2] \cdot \begin{bmatrix} 1 & 4 \\ 3 & 4 \end{bmatrix} = [A_{60}]$, $[A_2] \cdot \begin{bmatrix} 1 & 1 \\ 2 & 4 \end{bmatrix} = [A_{111}]$, $[A_2] \cdot \begin{bmatrix} 1 & 3 \\ 4 & 4 \end{bmatrix} = [A_{98}]$, and $[A_2] \cdot \begin{bmatrix} 1 & 2 \\ 1 & 4 \end{bmatrix} = [A_{75}]$.

After forming $A(X^{p,q})$ and calculating its eigenvalues we find that 4 and -4 are both eigenvalues with multiplicity 1. The degree of each vertex is 4, and there are no loops or multiple edges. Thus, $X^{p,q}$ is a connected, 4-regular, simple, bipartite graph. Furthermore, for every non-trivial eigenvalue λ_i , we find $|\lambda_i| \leq 3 \leq 2\sqrt{4-1}$. Thus, the resulting graph is Ramanujan.

For a fixed p , S_p remains constant as q varies. As we will see below, if $q > 2\sqrt{p}$, then $|S_{p,q}| = |S_p| = p + 1$. Thus as q varies, the regularity of $X^{p,q}$ remains equal to $p + 1$, and the quaternion Cayley construction can be used to generate infinitely many $p + 1$ regular graphs.

2.3. Properties of Quaternion Cayley Graphs

Theorem 5. *Given distinct odd primes p and q , with $p \geq 5, q > p^8$, the Cayley graphs $X^{p,q}$ are $(p + 1)$ -regular, connected, Ramanujan graphs. Furthermore,*

- If $\left(\frac{p}{q}\right) = 1$ then $X^{p,q}$ is non-bipartite, with $|V(X^{p,q})| = \frac{q(q^2-1)}{2}$.
- If $\left(\frac{p}{q}\right) = -1$ then $X^{p,q}$ is bipartite, with $|V(X^{p,q})| = q(q^2 - 1)$.

The $|V(X^{p,q})|$ follows directly from the cardinality of $PGL_2(q)$ and $PSL_2(q)$. It remains to prove:

1. $X^{p,q}$ is $(p + 1)$ -regular, i.e. that $|S_{p,q}| = p + 1$
2. $X^{p,q}$ is connected, or equivalently that $S_{p,q}$ generates $PSL_2(q)$ when $\left(\frac{p}{q}\right) = 1$, and $PGL_2(q)$ when $\left(\frac{p}{q}\right) = -1$.
3. $X^{p,q}$ is bipartite when $\left(\frac{p}{q}\right) = 1$, and non-bipartite when $\left(\frac{p}{q}\right) = -1$.
4. $X^{p,q}$ is Ramanujan

The proof of (4) relies on deep number theoretic results and is beyond the scope of this paper. We have already seen that if q is sufficiently larger than p , then $\tau_q(S_p) = S_p$. Since ψ_q is an isomorphism, $|\psi_q \circ \tau_q(S_p)| = |\tau_q(S_p)|$. Suppose A , and B are elements of $\psi_q \circ \tau_q(S_p)$ such that $A \neq B$ and $\phi(A) = \phi(B)$. Thus, there exists an element $\lambda \in \mathbf{Z}/q\mathbf{Z}$ such that

$$\det(A) = \lambda^2 \det(B). \quad (2.15)$$

Since A and B are the images of elements in S_p , it follows that $\det(A) = \det(B) = p$. Thus, equation 2.15 implies $\lambda^2 p = p$. Thus, $\lambda = \pm 1$, which implies $A = B$, or $A = -B$. The first case contradicts our assumption that $A \neq B$, the second case contradicts our assumption that both A , and B are elements of $\psi_q \circ \tau_q(S_p)$. Therefore, for all $A, B \in \psi_q \circ \tau_q(S_p)$, if $A \neq B$ then $\phi(A) \neq \phi(B)$ which implies $|\phi \circ \psi_q \circ \tau_q(S_p)| = |S_p| = p + 1$, assuming q is sufficiently large. Thus, $X^{p,q}$ is $(p + 1)$ -regular.

2.4. Proof that $X^{p,q}$ is connected

Theorem 6. For $p \geq 5, q > p^8$, $X^{p,q}$ is connected.

Proof. To prove $X^{p,q}$ is connected, it suffices to show $S_{p,q}$ generates $PSL_2(q)$ when $\left(\frac{p}{q}\right) = 1$, and $PGL_2(q)$ when $\left(\frac{p}{q}\right) = -1$.

Definition. Let

$$Z_q = \{\alpha \in \mathbf{H}(\mathbf{F}_q)^\times \mid \alpha = \bar{\alpha}\}, \quad (2.16)$$

i.e. Z_q is the set of real elements in $\mathbf{H}(\mathbf{F}_q)^\times$.

Definition. For all $\alpha, \beta \in \Lambda'$, define the equivalence relation \sim as follows.

$$\alpha \sim \beta \leftrightarrow p^m \alpha = \pm p^n \beta. \quad (2.17)$$

Let $\Lambda = \Lambda' / \sim$. Let Q be the quotient map from $\Lambda' \rightarrow \Lambda$.

From (2.5), we see that $\psi_q(\alpha)$ is a scalar matrix if and only if α is a real element of $\mathbf{H}(\mathbf{F}_q)^\times$. This implies $\psi_q(Z_q) = \ker(\phi)$. Thus, ψ_q descends to an isomorphism $\beta : \mathbf{H}(\mathbf{F}_q)^\times / \mathbf{Z}_q \rightarrow \mathbf{PGL}_2(q)$. Define $\pi_q : \Lambda \rightarrow \mathbf{H}(\mathbf{F}_q)^\times / \mathbf{Z}_q$, such that for all $\alpha \in S_p$, if $\tau_q(\alpha) \in Z_q$, then $Q(\alpha) \in \ker(\pi_q)$. Let $\Lambda(q) = \ker(\pi_q)$ and $T_{p,q} = \pi_q \circ Q(S_p)$.

To prove $X^{p,q}$ is connected, we first define the Cayley difference graphs $X(\Lambda, Q(S_p))$ and $Y^{p,q} = X(\Lambda/\Lambda(q), T_{p,q})$. From the previous definitions we have the following commutative diagram:

$$\begin{array}{ccccc} S_p \subset \Lambda' & \xrightarrow{\tau_q} & \mathbf{H}(\mathbf{F}_q)^\times & \xrightarrow{\psi_q} & GL_2(q) \\ \downarrow Q & & \downarrow & & \downarrow \phi \\ Q(S_p) \subseteq \Lambda & \xrightarrow{\pi_q} & T_{p,q} \subseteq \mathbf{H}(\mathbf{F}_q)^\times / \mathbf{Z}_q & \xrightarrow{\beta} & S_{p,q} \subseteq PGL_2(q) \\ X(\Lambda, Q(S_p)) & & Y^{p,q} = X(\Lambda/\Lambda(q), T_{p,q}) & & X^{p,q} \end{array} \quad (2.18)$$

We show that $Y^{p,q}$ is connected, and then use this fact to prove $X^{p,q}$ is also connected.

Claim 2. $X(\Lambda, Q(S_p))$ is the $(p+1)$ -regular tree.

Proof.

Theorem 7. For all $\alpha \in \Lambda'$ with $N(\alpha) = p^k$, α has a unique factorization, $\alpha = \pm p^r w_m$, where r is a natural number, w_m is a reduced word of length m over S_p , and $2r + m = k$.

Let α be any element of Λ' . Under the equivalence relation \sim , α is equivalent to some reduced word over S_p . Thus, $Q(S_p)$ generates Λ , which implies $X(\Lambda, Q(S_p))$ is connected. Furthermore, if $\alpha \sim \beta$, then $p^m \alpha = \pm p^n \beta$. Without loss of generality, assume $n > m$. By theorem (7), $\alpha = \pm p^{n-m} \beta$, implies $\alpha = \pm p^{r_\alpha} w_{m_\alpha} = \pm p^{n-m+r_\beta} w_{m_\beta}$.

Since this factorization is unique, $p^{n-m+r\beta} = p^{r\alpha}$ and $w_{m_\alpha} = w_{m_\beta}$. If α , and β are elements of S_p , then $N(\alpha) = N(\beta) = p$, and $N(\alpha) = N(\pm p^{n-m}\beta) = N(\pm p^{n-m})N(\beta) = N(\pm p^{n-m})p$. Thus, $N(\pm p^{n-m}) = 1$, which implies $\alpha = \pm\beta$. By (2.4), if $\alpha \in S_p$, then $-\alpha \notin S_p$. Therefore, if α , and β are elements of S_p , and $\alpha \sim \beta$, then $\alpha = \beta$. Thus $|Q(S_p)| = |S_p| = p + 1$. $X(\Lambda, Q(S_p))$ is $(p + 1)$ -regular.

To prove $X(\Lambda, Q(S_p))$ is a tree, assume it contains a cycle, and show a contradiction. Suppose $X(\Lambda, Q(S_p))$ contains a cycle $x_0, x_1, \dots, x_g = x_0$ of length $g \geq 3$. Assume $x_0 = [1]$. Thus, $x_1 = x_0[s_1] = [s_1]$, $x_2 = x_1[s_2] = [s_1s_2]$, ..., and $x_g = [s_1s_2\dots s_g] = [1]$ for some word $s_1s_2\dots s_g$, of length g in S_p . Thus, $1p^m = \pm p^n s_1s_2\dots s_g$. This contradicts the uniqueness of the factorization of α for every α in Λ' . Thus, $X(\Lambda, Q(S_p))$ contains no cycles of length ≥ 3 . $X(\Lambda, Q(S_p))$ is a tree. \square

Since $\ker(\pi_q) = \Lambda(q)$, it follows that $\text{Im}(\pi_q) \cong \Lambda/\Lambda(q)$. Furthermore, since $Q(S_p)$ generates Λ , $T_{p,q} = \pi_q(Q(S_p))$ generates $\Lambda/\Lambda(q)$. From (2.18), $S_{p,q} = \beta(T_{p,q})$. Thus, $S_{p,q}$ generates $\beta(\Lambda/\Lambda(q))$. To prove $S_{p,q}$ generates $PSL_2(q)$ when $\left(\frac{p}{q}\right) = 1$, and $PGL_2(q)$ when $\left(\frac{p}{q}\right) = -1$, it suffices to show

$$\beta(\Lambda/\Lambda(q)) = \begin{cases} PSL_2(q) & \text{if } \left(\frac{p}{q}\right) = 1 \\ PGL_2(q) & \text{if } \left(\frac{p}{q}\right) = -1 \end{cases} \quad (2.19)$$

Let $H = \beta(\Lambda/\Lambda(q)) \cap PSL_2(q)$. To prove (2.19) when $\left(\frac{p}{q}\right) = 1$, it suffices to show $H = PSL_2(q)$.

When $\left(\frac{p}{q}\right) = -1$, $S_{p,q} \subset PGL_2(q) - PSL_2(q)$ (see the proof of lemma 1). From the cardinality of $PGL_2(q)$ and $PSL_2(q)$, it follows that $PSL_2(q)$ is a subgroup of $PGL_2(q)$ of index 2. The two cosets of $PSL_2(q)$ partition $PGL_2(q)$. Suppose $S_{p,q}$ generates $PSL_2(q)$. If there exists an element $\alpha \in S_{p,q}$ such that $\alpha \notin PSL_2(q)$, then $\alpha PSL_2(q) = PGL_2 - PSL_2(q)$. This would imply that $S_{p,q}$ generates all of $PGL_2(q)$. If $\left(\frac{p}{q}\right) = -1$, such an α exists. Thus, in the $\left(\frac{p}{q}\right) = -1$ case, it also suffices to show $H = \beta(\Lambda/\Lambda(q)) \cap PSL_2(q) = PSL_2(q)$. The proof that $H = PSL_2(q)$ follows from the following theorem.

Theorem 8. *If p is prime and H is a proper subgroup of $PSL_2(q)$ with $|H| > 60$, then H is metabelian.*

Thus, if $|H| > 60$ and H is not metabelian, then H is not proper, i.e. $H = PSL_2(q)$. We can prove $|H| > 60$ using the assumption $p \geq 5, q > p^8$, and the following two observations:

$$1. |PGL_2(q)| \geq |\beta(\Lambda/\Lambda(q)) \cdot PSL_2(q)| = \frac{|\beta(\Lambda/\Lambda(q))| \cdot |PSL_2(q)|}{|H|}$$

$$\text{where } \beta(\Lambda/\Lambda(q)) \cdot PSL_2(q) = \{ab : a \in \beta(\Lambda/\Lambda(q)) \text{ and } b \in PSL_2(q)\}$$

$$2. |\beta(\Lambda/\Lambda(q))| = |Y^{p,q}| \geq \frac{p}{q}$$

We use the following result to prove H is not metabelian.

Lemma 2. *If G is metabelian, then $[[q_1, g_2], [g_3, g_4]] = 1, \forall g_1, g_2, g_3, g_4 \in G$.*

If $\left(\frac{p}{q}\right) = 1$ Chose h_1, h_2, h_3 , and $h_4 \in H$ as follows:

1. let h_1 be any element of $S_{p,q}$
2. $h_2 \neq h_1^{\pm 1}, h_2 \in S_{p,q}$
3. $h_3 = h_1$
4. $h_4 \notin \{h_1^{\pm 1}, h_2^{\pm 1}\}, h_4 \in S_{p,q}$

Thus, $[[h_1, h_2], [h_3, h_4]]$ is a reduced word of length 16 in $S_{p,q}$. The preimage of this word is a reduced word of length 16 in $T_{p,q}$. If $[[h_1, h_2], [h_3, h_4]] = [1]$, then the preimage = $[1]$ in $T_{p,q}$. Using an arguement mirroring that used in the proof of claim (2), we can show this word of length 16 in $T_{p,q}$ corresponds to a cycle of length ≤ 16 in $Y^{p,q}$. Similarly, if $\left(\frac{p}{q}\right) = -1$, we can chose $h_1, h_2, h_3, h_4 \in H$ such that if $[[h_1, h_2], [h_3, h_4]] = [1]$, then there exists a cycle of length ≤ 24 in $Y^{p,q}$. We can prove the following lower bounds on the girth of $Y^{p,q}$

$$g(Y^{p,q}) \geq \begin{cases} 2 \log_p q & \text{if } \left(\frac{p}{q}\right) = 1 \\ 4 \log_p q - \log_p 4 & \text{if } \left(\frac{p}{q}\right) = -1 \end{cases} \quad (2.20)$$

Thus, if $p \geq 5, q > p^8$,

$$g(Y^{p,q}) \geq \begin{cases} 2 \log_p q > 16 & \text{if } \left(\frac{p}{q}\right) = 1 \\ 4 \log_p q - \log_p 4 > 24 & \text{if } \left(\frac{p}{q}\right) = -1 \end{cases}$$

Therefore, $[[h_1, h_2], [h_3, h_4]]$ can not equal $[1]$, which implies H is not metabelian. Thus, $H = PSL_2(q)$ and $S_{p,q}$ generates $PSL_2(q)$ when $\left(\frac{p}{q}\right) = 1$, and $PGL_2(q)$ when $\left(\frac{p}{q}\right) = -1$, which implies $X^{p,q}$ is connected. \square

2.5. Bipartite $X^{p,q}$

Theorem 9. $X^{p,q}$ is bipartite when $\left(\frac{p}{q}\right) = 1$, and non-bipartite when $\left(\frac{p}{q}\right) = -1$

Proof.

Lemma 3. If the Cayley graph $X(G, S)$ is connected, then $X(G, S)$ is bipartite if and only if there exists a homomorphism $\pi : G \rightarrow \{+1, -1\}$ such that $\pi(s) = -1$ for all $s \in S$

Proof. (\Leftarrow) Given $\pi : G \rightarrow \{+1, -1\}$ such that $\pi(S) = -1$, set $V_+ = \{x \in G \mid \pi(x) = 1\}$, and $V_- = \{x \in G \mid \pi(x) = -1\}$. If $e = g_1g_2$ is an edge in $E(X(G, S))$, then $g_1 = g_2s$ for some $s \in S$. Thus, $\pi(g_1) = \pi(g_2s) = \pi(g_2) \cdot \pi(s) = -\pi(g_2)$, which implies $g_1 \in V_\pm$ and $g_2 \in V_\mp$. Thus, V_+ and V_- form a bipartition of $V(X(G, S))$.

(\Rightarrow) If $X(G, S)$ is bipartite and connected, define

$$\pi(x) = \begin{cases} +1 & \forall x \in V_+ \\ -1 & \forall x \in V_- \end{cases} \quad \text{where } S \subseteq V_-$$

Since S generates G , it follows that for all x in G , $\pi(x) = -1^{l_s(x)}$, where $l_s(x)$ equals the length of the word in S equal to x . Thus, for all x and $y \in G$, $\pi(xy) = -1^{l_s(xy)} = -1^{l_s(x)+l_s(y)} = -1^{l_s(x)} \cdot -1^{l_s(y)} = \pi(x) \cdot \pi(y)$ \square

If $\left(\frac{p}{q}\right) = 1$, then $X^{p,q} = X(PSL_2(q), S_{p,q})$. $PSL_2(q)$ is simple for all $q \geq 5$, i.e. the only normal subgroups of $PSL_2(q)$ are $\{1\}$ and $PSL_2(q)$. Thus, every group homomorphism on $PSL_2(q)$ must be constant or 1-1. There does not exist a homomorphism $\pi : PSL_2(q) \rightarrow \{\pm 1\}$. $X^{p,q}$ is not bipartite.

If $\left(\frac{p}{q}\right) = -1$, then $X^{p,q} = X(PGL_2(q), S_{p,q})$, where $S_{p,q} \subset PGL_2(q) - PSL_2(q)$. Thus, the isomorphism $PGL_2(q)/PSL_2(q) \cong \{\pm 1\}$ maps S to -1. $X^{p,q}$ is bipartite. \square

We have shown that the quaternion Cayley construction yields connected, $(p+1)$ -regular graphs, which are bipartite in the $\left(\frac{p}{q}\right) = -1$ case, and non-bipartite in the $\left(\frac{p}{q}\right) = 1$ case.

The quaternion Cayley graph construction, in conjunction with theorem 5, allows us to generate k -regular, simple, Ramanujan graphs. Unfortunately, since $|PSL_2(q)| = \frac{q(q^2-1)}{2}$, and $|PGL_2(q)| = q(q^2 - 1)$, the requirement that $p \geq 5$, and $q > p^8$ leads to graphs with very large vertex sets. Large $|V(X^{p,q})|$ makes it computationally costly to generate the adjacency matrix and analyze its spectrum directly. While theorem 5 allows us to determine whether a graph is Ramanujan without calculating its spectrum, the spectrum of the adjacency matrix is still of interest. Is it described by some universal distribution function? How are the spacings of consecutive eigenvalues distributed? To answer these questions we need all eigenvalues of $X^{p,q}$.

3. RANDOM GRAPHS

While the quaternion Cayley graph construction generates $(p+1)$ -regular families of Ramanujan graphs, it does not provide a construction for k -regular families if k is arbitrary. In fact, $k = 7$ is the first value of k for which there is no known explicit construction.

Our approach to this open problem of constructing a family of 7-regular Ramanujan graphs has been to examine random¹ 7-regular graphs. By determining which of these graphs are Ramanujan we hope to find characteristics which might advance attempts at constructing 7-regular families of Ramanujan graphs.

3.1. Construction of Random, Simple, 7-Regular Graphs

To construct random 7-regular graphs, begin by taking the cycle graph on n vertices, which has adjacency matrix C . To this add two randomly permuted cycle graphs, each having n vertices, and one randomly permuted “toothpick” graph², also having n vertices. The toothpick graph is the 1-regular graph on $n = 2m$ vertices in which vertex v_1 is adjacent to vertex v_2 , v_3 is adjacent to v_4 , v_5 is adjacent to v_6 , ..., v_{2m-1} is adjacent to v_{2m} (see figure 3.1). To generate the randomly permuted cycle and toothpick graphs, use Matlab to find random permutations on n elements and express these permutations as n by n matrices P_i . The cycle and the toothpick graphs are

¹By “random” I mean those graphs whose construction depends on a randomly selected permutation. The explicit construction of these graphs will be given below.

²The toothpick graph is the graph on $n = 2m$ vertices whose adjacency matrix is given by

$$T = \begin{bmatrix} 0 & 1 & 0 & 0 & \dots & 0 & 0 \\ 1 & 0 & 0 & 0 & \dots & 0 & 0 \\ 0 & 0 & 0 & 1 & \dots & 0 & 0 \\ 0 & 0 & 1 & 0 & \dots & 0 & 0 \\ \dots & \dots & \dots & \dots & \dots & \dots & \dots \\ 0 & 0 & 0 & 0 & \dots & 0 & 1 \\ 0 & 0 & 0 & 0 & \dots & 1 & 0 \end{bmatrix}$$

The adjacency matrix of the cycle graph is given by

$$C = \begin{bmatrix} 0 & 1 & 0 & 0 & \dots & 0 & 1 \\ 1 & 0 & 1 & 0 & \dots & 0 & 0 \\ 0 & 1 & 0 & 1 & \dots & 0 & 0 \\ \dots & \dots & \dots & \dots & \dots & \dots & \dots \\ 0 & 0 & 0 & 0 & \dots & 0 & 1 \\ 1 & 0 & 0 & 0 & \dots & 1 & 0 \end{bmatrix}$$

permuted by taking $P_i^T * C * P_i$ and $P_j^T * T * P_j$ respectively. Thus, the adjacency matrix of the resulting 7-regular graph is given by

$$A = C + P_1^T * C * P_1 + P_2^T * C * P_2 + P_3^T * T * P_3. \quad (3.1)$$

Example. To illustrate the process, let's examine the construction of a 7-regular graph on 6 vertices.

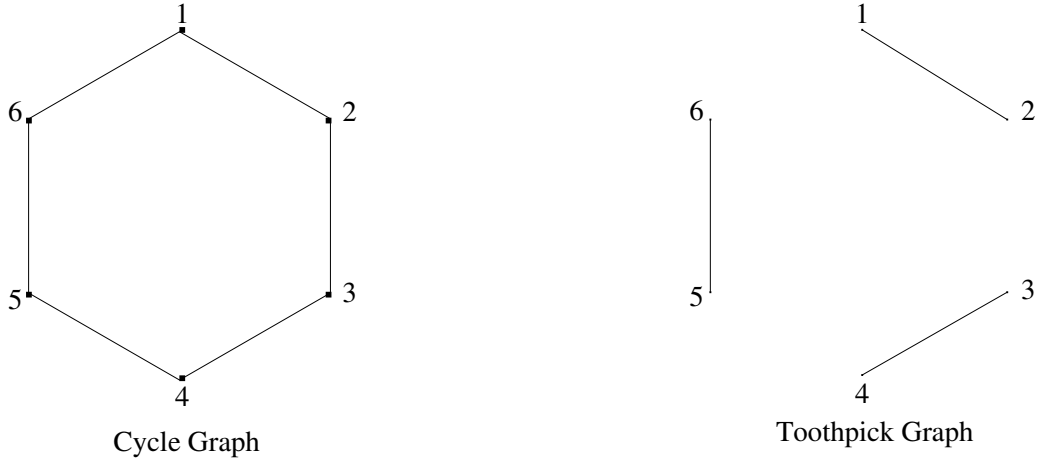


FIGURE 3.1. Cycle and Toothpick Graphs on 6 vertices

Using Matlab, we find the random permutations $p_1 = (1246)(3)(5)$, $p_2 = (124563)$, and $p_3 = (132465)$ corresponding to the permutation matrices

$$P_1 = \begin{bmatrix} 0 & 1 & 0 & 0 & 0 & 0 \\ 0 & 0 & 0 & 1 & 0 & 0 \\ 0 & 0 & 1 & 0 & 0 & 0 \\ 0 & 0 & 0 & 0 & 0 & 1 \\ 0 & 0 & 0 & 0 & 1 & 0 \\ 1 & 0 & 0 & 0 & 0 & 0 \end{bmatrix}, \quad P_2 = \begin{bmatrix} 0 & 1 & 0 & 0 & 0 & 0 \\ 0 & 0 & 0 & 1 & 0 & 0 \\ 1 & 0 & 0 & 0 & 0 & 0 \\ 0 & 0 & 0 & 0 & 1 & 0 \\ 0 & 0 & 0 & 0 & 0 & 1 \\ 0 & 0 & 1 & 0 & 0 & 0 \end{bmatrix}, \quad \text{and } P_3 = \begin{bmatrix} 0 & 0 & 1 & 0 & 0 & 0 \\ 0 & 0 & 0 & 1 & 0 & 0 \\ 0 & 1 & 0 & 0 & 0 & 0 \\ 0 & 0 & 0 & 0 & 0 & 1 \\ 1 & 0 & 0 & 0 & 0 & 0 \\ 0 & 0 & 0 & 0 & 1 & 0 \end{bmatrix}$$

Thus, the permuted cycles $P_1^T * C * P_1$, $P_2^T * C * P_2$, and the permuted toothpick graph $P_3^T * C * P_3$ are given by the adjacency matrices

$$\begin{bmatrix} 0 & 1 & 0 & 0 & 1 & 0 \\ 1 & 0 & 0 & 1 & 0 & 0 \\ 0 & 0 & 0 & 1 & 0 & 1 \\ 0 & 1 & 1 & 0 & 0 & 0 \\ 1 & 0 & 0 & 0 & 0 & 1 \\ 0 & 0 & 1 & 0 & 1 & 0 \end{bmatrix}, \quad \begin{bmatrix} 0 & 0 & 0 & 1 & 1 & 0 \\ 0 & 0 & 1 & 1 & 0 & 0 \\ 0 & 1 & 0 & 0 & 0 & 1 \\ 1 & 1 & 0 & 0 & 0 & 0 \\ 1 & 0 & 0 & 0 & 0 & 1 \\ 0 & 0 & 1 & 0 & 1 & 0 \end{bmatrix}, \quad \text{and } \begin{bmatrix} 0 & 0 & 0 & 0 & 1 & 0 \\ 0 & 0 & 0 & 0 & 0 & 1 \\ 0 & 0 & 0 & 1 & 0 & 0 \\ 0 & 0 & 1 & 0 & 0 & 0 \\ 1 & 0 & 0 & 0 & 0 & 0 \\ 0 & 1 & 0 & 0 & 1 & 0 \end{bmatrix}$$

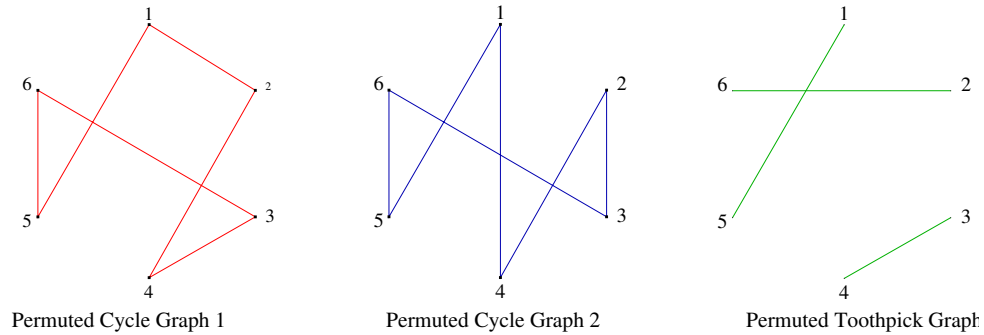


FIGURE 3.2. Permutated Cycle and Toothpick Graphs on 6 Vertices

respectively, and are shown in figure 3.2. The resulting 7 regular graph is given by the adjacency matrix

$$A = C + P_1^T * C * P_1 + P_2^T * C * P_2 + P_3^T * T * P_3 = \begin{bmatrix} 0 & 2 & 0 & 1 & 3 & 1 \\ 2 & 0 & 2 & 2 & 0 & 1 \\ 0 & 2 & 0 & 3 & 0 & 2 \\ 1 & 2 & 3 & 0 & 1 & 0 \\ 3 & 0 & 0 & 1 & 0 & 3 \\ 1 & 1 & 2 & 0 & 3 & 0 \end{bmatrix}$$

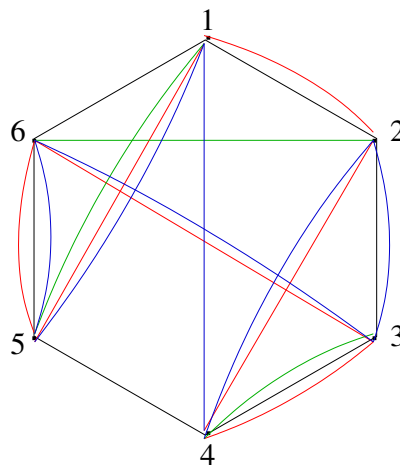


FIGURE 3.3. Resulting 7 Regular Graph

In the previous example we see that the resulting 7-regular graph is actually a multigraph. In practice, this construction technique results in multigraphs more often

than not. When used to construct 7-regular graphs on 2000 vertices, approximately 1 simple graph is generated for every 10,000 multigraphs. Fortunately, for large n , even small samples of simple, 7-regular graphs can be used to study the distribution of the eigenvalues³. To determine which of the generated 7-regular graphs were simple, the maximum entry of the adjacency matrix was checked, and only graphs with maximum entry = 1 were included in the sample.

3.2. Distribution of Eigenvalues

Histograms of the eigenvalues of our generated simple, 7-regular graphs for various n provide an empirical estimate of the probability density function. These eigenvalue densities correspond to the McKay density

$$f_k(x) = \begin{cases} \frac{k\sqrt{4(k-1)-x^2}}{2\pi(k^2-x^2)} & \text{when } |x| \leq 2\sqrt{k-1} \\ 0 & \text{otherwise} \end{cases} \quad (3.2)$$

(see figure 3.4).

McKay proved the following theorem[3]:

Theorem 10. *Given a sequence X_1, X_2, \dots of k -regular, simple, graphs for some $k \geq 2$, let $|X_n|$ denote the number of vertices in graph X_n and $c_r(X_n)$ the number of r -cycles⁴. If $|X_n| \rightarrow \infty$ as $n \rightarrow \infty$, and*

$$\lim_{n \rightarrow \infty} \frac{c_r(X_n)}{|X_n|} = 0 \quad \forall r \geq 3 \quad (3.3)$$

the limiting probability density distribution function for the eigenvalues of X_n as $n \rightarrow \infty$ is given by equation (3.2).

3.3. Distribution of Eigenvalue Spacings

One of the basic objects of Random Matrix Theory (RMT) is the distribution of the spacings between consecutive⁵ eigenvalues. Of particular interest is the distribution of scaled eigenvalue spacings for the bulk of the spectrum, where the spacings are scaled to mean 1 and integrated density 1. The density function describing this distribution in the limit $|X_n| \rightarrow \infty$ is called the bulk scaling limit. The bulk of the spectrum

³The empirical distributions generated from samples as small as 20 graphs were observed to approximate known distributions well.

⁴An r -cycle is a closed walk of length r that has no repeated edges or vertices (except for the starting and ending vertex)

⁵Consecutive under the eigenvalue ordering $\mu_0 \geq \mu_1 \geq \dots \geq \mu_{n-1}$

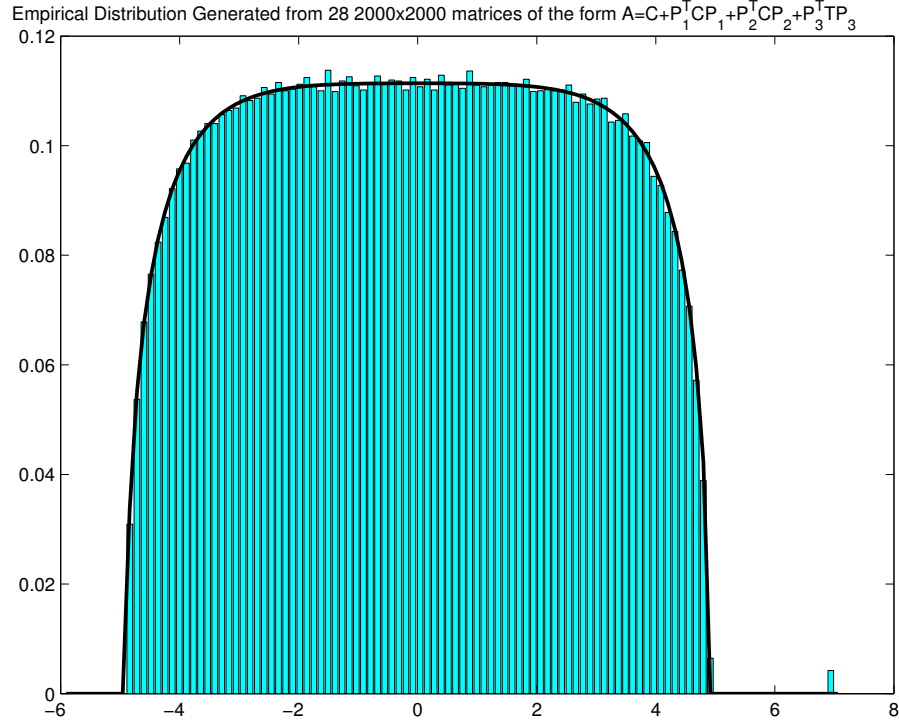


FIGURE 3.4. Eigenvalue Distribution for Simple, 7-Regular Graphs vs. the McKay density $f_k(x)$

refers to the scaled eigenvalues lying near the center of the spectrum, i.e. away from the edges.

One commonly studied ensemble in Random Matrix Theory is the Gaussian orthogonal ensemble (GOE). The GOE consists of $N \times N$ symmetric matrices whose components are independent⁶, random variables of mean zero and standard deviation one. The distribution of scaled eigenvalues⁷ for the Gaussian orthogonal ensemble is described by the *Wigner semicircle distribution*, ρ_W [5].

$$\rho_W(y) = \begin{cases} \frac{2}{\pi} \sqrt{1 - y^2} & \text{when } |y| \leq 1 \\ 0 & \text{otherwise} \end{cases} \quad (3.4)$$

The bulk scaling limit is known for the GOE, and is approximated by the *Wigner surmise*, ϱ_W .

$$\varrho_W(s) = \frac{\pi}{2} \exp\left(-\frac{\pi}{4}s^2\right) \quad (3.5)$$

⁶The elements are independent up to the requirement that the matrix be symmetric. Thus, once the i_j^{th} element has been determined, the j_i^{th} element is also determined.

⁷Scaled so that the integrated density is 1, and all scaled eigenvalues lie in $[-1,1]$

Examining equation 3.2, one finds that by using the change of variables $x = 2\sqrt{k-1}y$, we can scale f_k so that it has support $[-1,1]$.

$$f_k(x)dx \rightarrow \tilde{f}_k(y)dy \quad \text{where} \quad \tilde{f}_k(y) = \begin{cases} \frac{2k(k-1)\sqrt{1-y^2}}{\pi(k^2-4(k-1)y^2)} & \text{when } |y| \leq 1 \\ 0 & \text{otherwise} \end{cases} \quad (3.6)$$

Comparing equation 3.6 with equation 3.4 we find

$$\tilde{f}_k(y) = \left(\frac{k(k-1)}{k^2-4(k-1)y^2} \right) \cdot \rho_W(y)$$

Thus, the McKay density is a distortion of the Wigner semicircle density, and in the limit $k \rightarrow \infty$, $\tilde{f}_k(y) \rightarrow \rho_W(y)$. The factor $\left(\frac{k(k-1)}{k^2-4(k-1)y^2} \right)$ is plotted in figure 3.5 for various values of k . From figure 3.5 we immediately observe that the distortion factor $\rightarrow 1$ as $k \rightarrow \infty$, and the distortion is always greatest near the edges of the spectrum.

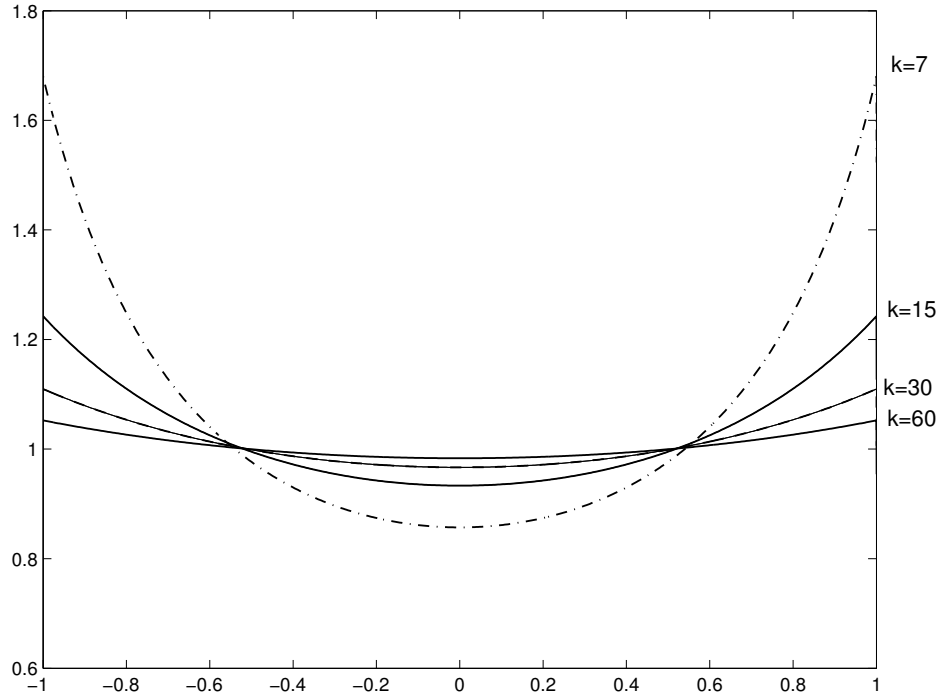


FIGURE 3.5. $\left(\frac{k(k-1)}{k^2-4(k-1)y^2} \right)$ plotted over the support of $\tilde{f}_k(y)$ for various k

Since the distribution of scaled eigenvalues for the GOE differs from the McKay density by the the distortion factor $\left(\frac{k(k-1)}{k^2-4(k-1)y^2} \right)$, which is approximately 1 over

the bulk of the spectrum, it seems likely that the bulk scaling limit for eigenvalue distributions described by the McKay density, will be the same as that for the GOE. In figure 3.6 the empirical distribution of scaled eigenvalue spacings for the bulk of the spectrum of our random, simple, 7-regular graphs, is plotted against the Wigner Surmise.

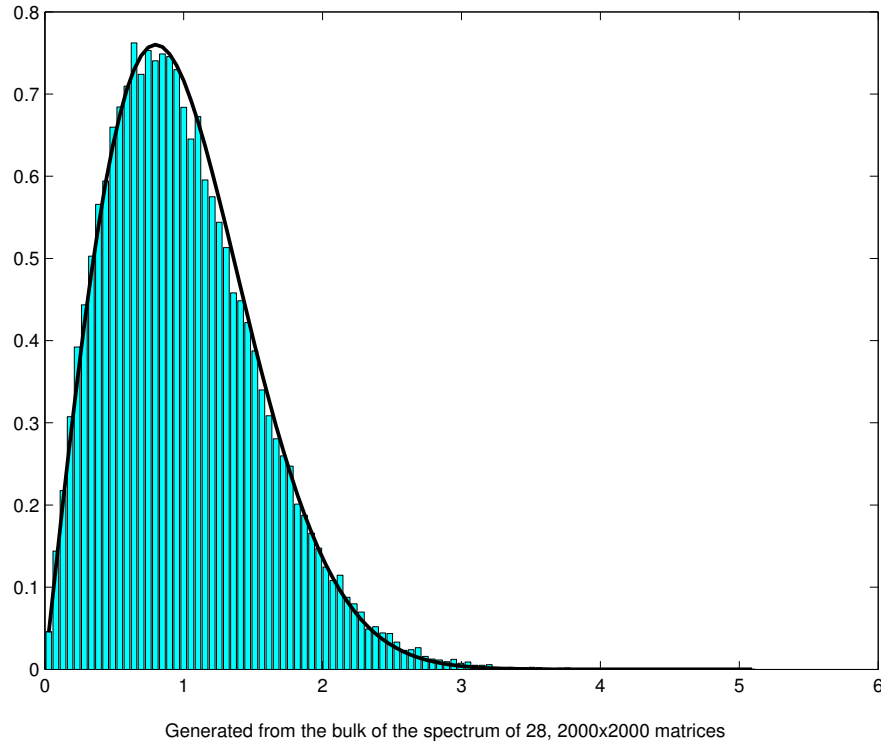


FIGURE 3.6. Distribution of scaled eigenvalue spacings for our simple 7-regular graphs vs. the Wigner surmise

3.4. Random, 7-regular, Ramanujan Graphs

Recall that a k -regular graph is Ramanujan if and only if the absolute value of the associated eigenvalues, μ_1 and μ_{n-1} , are $\leq 2\sqrt{k-1}$ (see definition 1.6). Thus,

$$P(X \text{ is Ramanujan}) = P(|\mu_1| \leq 2\sqrt{k-1}) \cap (|\mu_{n-1}| \leq 2\sqrt{k-1}).$$

Examining the percentage of randomly generated 7-regular graphs for which $|\mu_1| \leq 2\sqrt{k-1}$, and the percentage for which $|\mu_{n-1}| \leq 2\sqrt{k-1}$, and comparing these per-

centages to the percent Ramanujan for various n , it appears that

$$\begin{aligned} P(X \text{ is Ramanujan}) &= P((|\mu_1| \leq 2\sqrt{k-1}) \cap (|\mu_{n-1}| \leq 2\sqrt{k-1})) \\ &= P(|\mu_1| \leq 2\sqrt{k-1}) \cdot P(|\mu_{n-1}| \leq 2\sqrt{k-1}) \end{aligned} \quad (3.7)$$

which suggests that μ_1 and μ_{n-1} are independent random variables (see table 3.1).

n	$P(\mu_1 \leq 2\sqrt{6})$	$P(\mu_{n-1} \leq 2\sqrt{6})$	$P(\mu_1 \leq 2\sqrt{6}) \times P(\mu_{n-1} \leq 2\sqrt{6})$	% Ramanujan
200	92%	77%	71%	71%
400	90%	78%	70%	70%
500	91%	78%	71%	71%
800	89%	78%	70%	69%
1000	89%	80%	71%	72%
2000	88%	80%	71%	71%

TABLE 3.1. Comparison of the distribution of μ_1 , μ_{n-1} , and the percentage of graphs which are Ramanujan for various matrix sizes n

Furthermore, it appears that for large n , approximately 71% of the generated⁸ random graphs are Ramanujan. The reason why Ramanujan graphs should consistently account for $\approx 71\%$ of the generated samples is not understood. To examine this phenomenon further, we study the distribution of μ_1 and μ_{n-1} .

3.5. Edge Behavior

While sample sizes as small as 20 matrices were sufficient for examining the distribution of eigenvalues and eigenvalue spacings, determining the distribution of μ_1 and μ_{n-1} requires large samples. Generating these large samples of 7-regular, simple, random graphs on n vertices is computationally infeasible, however we can generate large samples of 7-regular, random multigraphs. To this end, I generated random, 7-regular graphs of the form

$$A = T + P_1^T * T * P_1 + P_2^T * T * P_2 + P_3^T * T * P_3 + P_4^T * T * P_4 + P_5^T * T * P_5 + P_6^T * T * P_6 \quad (3.8)$$

where T is the adjacency matrix of the toothpick graph on n vertices and P_i are random permutation matrices⁹. In the limit $|X_n| \rightarrow \infty$, the distribution of scaled eigenvalues for these random graphs \rightarrow the McKay density $f_k(x)$, [2].

⁸Data in table 3.1 is from random graphs generated according to equation 3.8.

⁹These numerical experiments were done prior to those examining the distribution of scaled eigenvalues and eigenvalue spacings for random 7-regular, simple, graphs. The construction method used in these latter experiments, 3.1, was chosen to increase the probability of generating a simple graph.

Let $\langle \mu_i^{(n)} \rangle$ denote the mean value of the i^{th} eigenvalue for matrices of size $n \times n$. Let $\sigma_i^{(n)}$ denote the standard deviation in μ_i . Examining the mean and standard deviation of μ_1 and μ_{n-1} for various n we find $\langle \mu_1 \rangle + \sigma_1$ approaches $2\sqrt{k-1}$ from the left, while $|\langle \mu_{n-1} \rangle - \sigma_{n-1}|$ approaches $2\sqrt{k-1}$ from the right (see table 3.2). To find density functions describing μ_1 and μ_{n-1} in the limit as $n \rightarrow \infty$, we need to scale μ_1 and μ_{n-1} such that the distribution of the resulting scaled variable does not depend on n .

n	$\langle \mu_1 \rangle$	σ_1	$2\sqrt{6} - \langle \mu_1 \rangle$	$2\sqrt{6} - (\langle \mu_1 \rangle + \sigma_1)$
200	4.8021	0.0677	0.0969	0.0292
400	4.8434	0.0420	0.0556	0.0136
500	4.8509	0.0357	0.0481	0.0124
600	4.8576	0.0316	0.0414	0.0098
800	4.8663	0.0262	0.0327	0.0065
1000	4.8712	0.0225	0.0278	0.0053
2000	4.8824	0.0138	0.0166	0.0028
n	$\langle \mu_{n-1} \rangle$	σ_{n-1}	$-2\sqrt{6} - \langle \mu_{n-1} \rangle$	$-2\sqrt{6} - (\langle \mu_{n-1} \rangle - \sigma_{n-1})$
200	-4.8522	0.0651	-0.0468	0.0183
400	-4.8683	0.0412	-0.0307	0.0105
500	-4.8721	0.0354	-0.0269	0.0085
600	-4.8751	0.0315	-0.0239	0.0076
800	-4.8792	0.0260	-0.0198	0.0062
1000	-4.8809	0.0223	-0.0181	0.0042
2000	-4.8873	0.0142	-0.0117	0.0025

TABLE 3.2. Position of $\langle \mu_1 \rangle$ and $\langle \mu_{n-1} \rangle$ relative to $\pm 2\sqrt{6}$ for various n . Data generated from samples of 5,000 matrices for each n .

Examining the log-log plots of $\langle \mu_1 - 2\sqrt{6} \rangle$ and $|\langle -\mu_{n-1} - 2\sqrt{6} \rangle|$ versus n , it appears that $\langle \mu_1 - 2\sqrt{6} \rangle$ and $\langle -\mu_{n-1} - 2\sqrt{6} \rangle$ scale like power laws (see figure 3.7). In particular, it appears that the mean of the scaled variables

$$S_1 = C_1 * n^{\beta_1}(\mu_1 - 2\sqrt{6}) \quad \text{and} \quad S_{n-1} = C_{n-1} * n^{\beta_{n-1}}(-\mu_{n-1} - 2\sqrt{6}) \quad (3.9)$$

will not depend on n if β_1 and β_{n-1} are properly chosen.

Under this scaling, a graph is Ramanujan if the associated scaled variables S_1 and S_{n-1} are both ≤ 0 . If μ_1 and μ_{n-1} are independent random variables, then so too are S_1 and S_{n-1} . Thus, if there exist density functions h_1 and h_2 , describing the distributions of S_1 and S_{n-1} in the limit $n \rightarrow \infty$, the percentage of graphs of type (3.8) that are Ramanujan should approach the constant value

$$\left(\int_{-\infty}^0 h_1(x) dx \right) \left(\int_{-\infty}^0 h_2(x) dx \right). \quad (3.10)$$

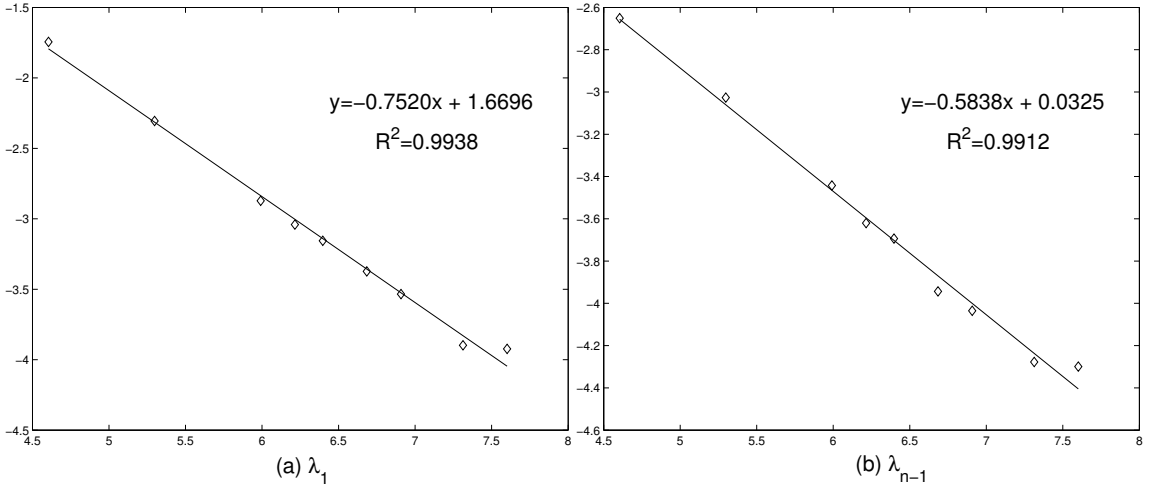


FIGURE 3.7. Log Log plot of $\langle \lambda_1 - 2\sqrt{6} \rangle$ and $|\langle -\lambda_{n-1} - 2\sqrt{6} \rangle|$ vs. matrix size n , as n ranges over the sizes 100, 200, 400, 500, 600, 800, 1000, 1500, and 2000 corresponding to samples of 1000, 1000, 1000, 1504, 1000, 1500, 1265, 7347, and 1000 matrices respectively.

Thus, for large n , we would expect to find the observed invariance in the percent Ramanujan.

3.6. Scaling Parameters and Distributions of S_1 and S_{n-1}

From equation (3.9) we see there are 4 scaling parameters, C_1 , C_{n-1} , β_1 , and β_{n-1} , which have to be determined in the definition of S_1 and S_{n-1} . The log log plots of $\langle \mu_1 - 2\sqrt{6} \rangle$ and $|\langle -\mu_{n-1} - 2\sqrt{6} \rangle|$ vs. n can be used to estimate the parameters β_1 and β_{n-1} . Unfortunately these plots are very sensitive to slight changes in the values $\langle \mu_1 - 2\sqrt{6} \rangle$ and $|\langle -\mu_{n-1} - 2\sqrt{6} \rangle|$. Since $\langle \mu_1 - 2\sqrt{6} \rangle$ and $|\langle -\mu_{n-1} - 2\sqrt{6} \rangle|$ are determined experimentally, there is a enough uncertainty in their measurements to significantly alter the estimation of β_1 and β_{n-1} .

Previous numerical studies examining the random 3-regular graphs $A = C + P_1^T * T * P_1$ and $A = T + P_1^T * T * P_1 + P_2^T * T * P_2$ suggest that for large n , the distributions of S_1 and S_{n-1} might be governed by the Tracy-Widom distributions f_4 and f_1 respectively. These density functions are related to the Gaussian orthogonal ensemble and the Gaussian symplectic ensemble (GSE) in random matrix theory. As previously discussed, the GOE consists of $N \times N$ symmetric matrices whose components are independent, Gaussian random variables. The GSE consists of $2N \times 2N$ self-dual hermitian matrices whose components are independent, real quaternion¹⁰,

¹⁰i.e. elements of $\mathbf{H}(\mathbf{R})$

Gaussian random variables. The density function f_1 describes the distribution of the scaled largest eigenvalue in the limit as $n \rightarrow \infty$ for the GOE. The largest eigenvalue is scaled according to the equation

$$S_{GOE} = \frac{N^{\frac{1}{6}}}{\sigma}(\mu_1 - 2\sigma\sqrt{N}) \quad (3.11)$$

where σ is the standard deviation of the Gaussian distribution. The density function f_4 describes the distribution of the scaled largest eigenvalue in the limit as $n \rightarrow \infty$ for the GSE. For the GSE, the scaled variable is given by

$$S_{GSE} = \frac{(2N + 1)^{\frac{1}{6}}}{\sigma^\circ}(\mu_1 - 2\sigma^\circ\sqrt{2N + 1}) \quad (3.12)$$

where $\frac{\sigma^\circ}{\sqrt{2}}$ is equal to the standard deviation of the Gaussian distribution [6]. The mean and standard deviation of f_1 and f_4 are given in table 3.3.

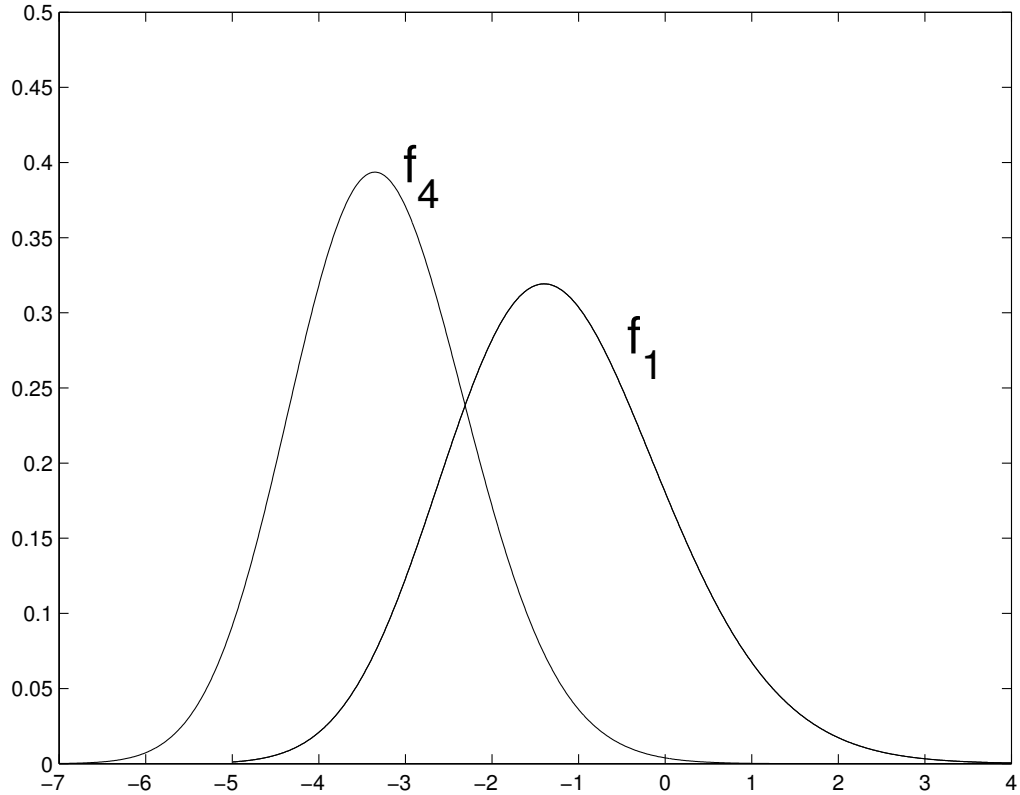


FIGURE 3.8. Plot of the Tracy-Widom distributions f_1 and f_4

Starting with the hypothesis that, given proper scaling parameters, the distribution of S_1 and S_{n-1} are given by f_4 and f_1 , parameters C_1 , C_{n-1} , β_1 , and β_{n-1} were

sought to minimize the difference between the distribution of S_1 and f_4 , and the distribution of S_{n-1} and f_1 , for large n . Starting with β_1 and β_{n-1} approximately equal to the values determined by the log-log plots (figure 3.7), C_1 and C_{n-1} were found by setting the mean of S_1 equal to the mean of f_4 , and the mean of S_{n-1} equal to that of f_4 . After several refinements, it appears that the difference between the cumulative distribution function (c.d.f.) of S_1 and that associated with f_4 , is minimized when f_4 is shifted by 2 to the right, $\beta_1 = \frac{3}{5}$, and $C_1 = \frac{3}{4}$. Similarly, the difference between the c.d.f. of S_{n-1} , and that associated with f_1 , is minimized when f_1 is shifted by $\frac{1}{8}$ to the right, $\beta_{n-1} = \frac{5}{8}$, and $C_{n-1} = \frac{4}{5}$. See figures 3.9 and 3.10.

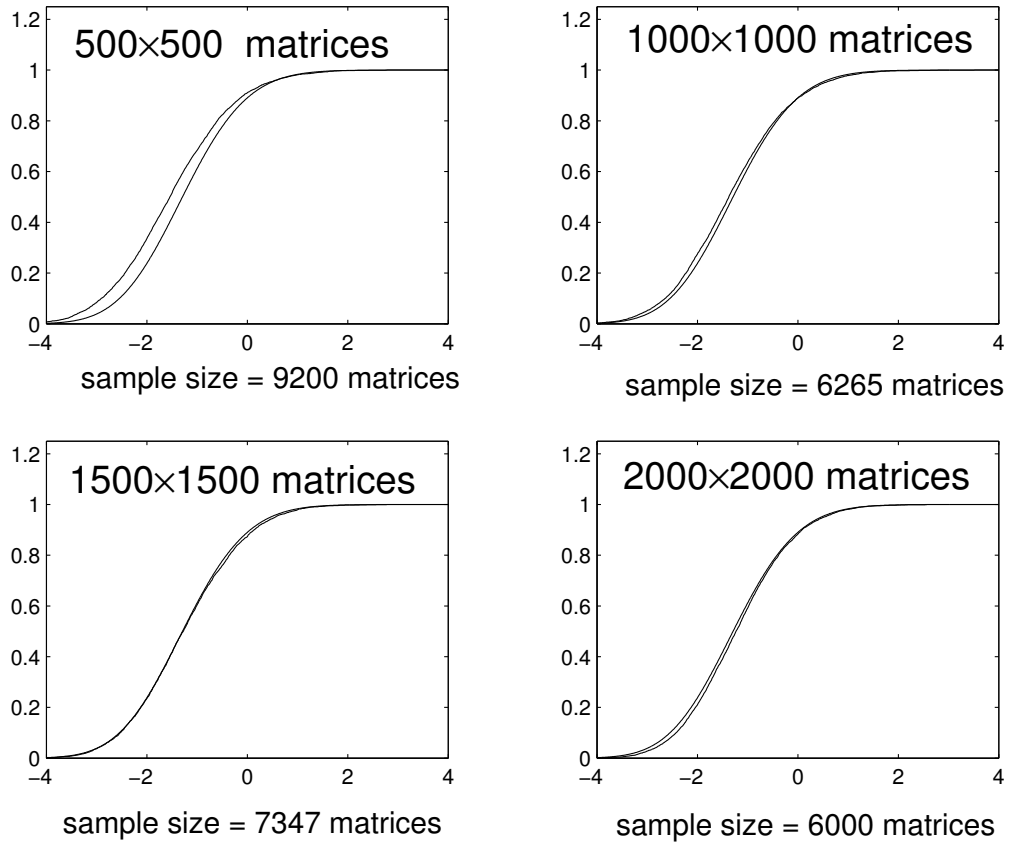


FIGURE 3.9. Empirical cumulative density function of S_1 plotted against the Tracy-Widom c.d.f., F_4 , for various values of n . F_4 is shifted by 2 to the right, and the scaling parameters are $\beta_1 = \frac{3}{5}$ and $C_1 = \frac{3}{4}$

If the distributions of

$$S_1 = \frac{3}{4} * n^{\frac{3}{5}}(\mu_1 - 2\sqrt{6}) \quad \text{and} \quad S_{n-1} = \frac{4}{5} * n^{\frac{5}{8}}(-\mu_{n-1} - 2\sqrt{6})$$

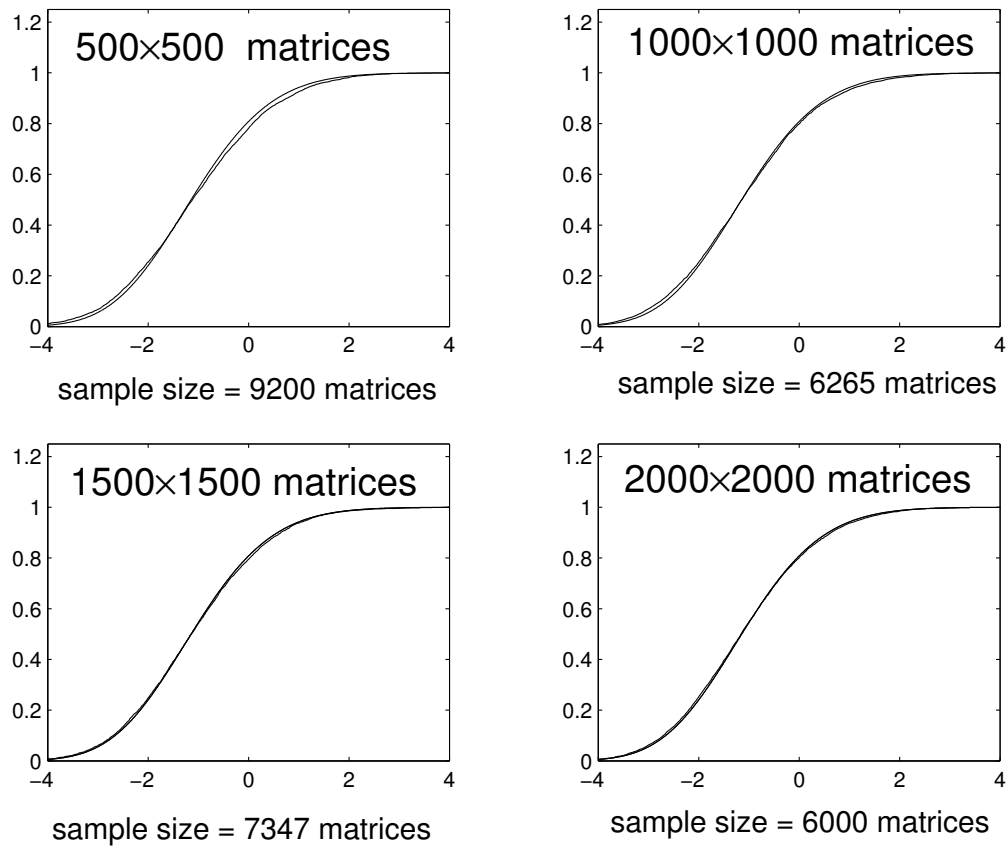


FIGURE 3.10. Empirical cumulative density function of S_{n-1} plotted against the Tracy-Widom c.d.f., F_1 , for various values of n . F_1 is shifted by $\frac{1}{8}$ to the right, and the scaling parameters are $\beta_{n-1} = \frac{5}{8}$ and $C_{n-1} = \frac{4}{5}$

are in fact described by the density functions f_4 shifted by 2, and f_1 shifted by $\frac{1}{8}$, then the percentage of Ramanujan graphs should approach the constant value

$$p = \left(\int_{-\infty}^{-\frac{1}{8}} f_1(x) dx \right) \left(\int_{-\infty}^{-2} f_4(x) dx \right). \quad (3.13)$$

A very rough estimate of the integrals in (3.13) gives

$$\int_{-\infty}^{-\frac{1}{8}} f_1(x) dx = 81\% \quad \text{and} \quad \int_{-\infty}^{-2} f_4(x) dx = 89\%$$

Thus, if our assumption that S_1 and S_{n-1} are described by the distributions f_4 and f_1 is correct, the percentage of graphs which are Ramanujan should approach the value

$81\% \cdot 89\% = 72\%$. This is not far from the observed percent Ramanujan and hence, seems to support our assumption about f_1 and f_4 .

3.7. Inconsistencies

While we can find $\beta_1, \beta_{n-1}, C_1$, and C_{n-1} such that the distributions of S_1 and S_{n-1} match the Tracy Widom distributions reasonably well for all examined n , do these known density functions really describe our empirical data? We note that

$$\frac{\langle S_1 \rangle}{\sigma_{S_1}} = \frac{\langle \lambda_1 - 2\sqrt{6} \rangle}{\sigma_1} \quad \text{and} \quad \frac{\langle S_{n-1} \rangle}{\sigma_{S_{n-1}}} = \frac{\langle -\lambda_{n-1} - 2\sqrt{6} \rangle}{\sigma_{n-1}}. \quad (3.14)$$

Thus, our scaling parameters β and C don't affect the ratios $\frac{\langle S_1 \rangle}{\sigma_{S_1}}$ and $\frac{\langle S_{n-1} \rangle}{\sigma_{S_{n-1}}}$. If f_4 and f_1 truly describe the distributions of S_1 and S_{n-1} respectively, then

$$\frac{\langle S_1 \rangle}{\sigma_{S_1}} = \frac{\langle f_4 \rangle}{\sigma_{f_4}} + C_{shift_4} \quad \text{and} \quad (3.15)$$

$$\frac{\langle S_{n-1} \rangle}{\sigma_{S_{n-1}}} = \frac{\langle f_1 \rangle}{\sigma_{f_1}} + C_{shift_1} \quad (3.16)$$

where C_{shift_1} and C_{shift_4} are the horizontal shifts in the Tracy Widom distributions.

Distribution	Mean, $\langle f_i \rangle$	Standard Deviation, σ_i	Ratio $\frac{\langle f_i \rangle}{\sigma_i}$	Ratio + C_{shift_i}
f_1	-1.2105	1.2660	-0.9562	-0.8312
f_4	-3.2674	1.0178	-3.2103	-1.2103

TABLE 3.3. Approximate Parameter Values of the Tracy Widom Distributions f_1 and f_4

While initial results suggested that the distribution of S_1 might fit the Tracy Widom distribution f_4 , shifted 2 units to the right, table (3.4) indicates this may not be the case. Not only is $\frac{\langle S_1 \rangle}{\sigma_{S_1}} \neq \frac{\langle f_4 \rangle}{\sigma_{f_4}} + 2$, the ratios $\frac{\langle S_1 \rangle}{\sigma_{S_1}}$ vary with n , casting doubt on our original hypothesis that $\langle \lambda_1 - 2\sqrt{6} \rangle \sim n^{-\beta_1}$. While the f_1 shifted by $\frac{1}{8}$ appeared to describe the distribution of S_{n-1} , the ratios in tables (3.4) and (3.3) show that f_1 would have to be shifted by approximately 1/4 in order for $\frac{\langle S_{n-1} \rangle}{\sigma_{S_{n-1}}} = \frac{\langle f_1 \rangle}{\sigma_{f_1}} + C_{shift_1}$. Thus far, no C_{n-1} and β_{n-1} have been found such that the distribution of S_{n-1} fits f_1 shifted by 1/4. The data in table (3.4) does indicate that $|\langle -\lambda_{n-1} - 2\sqrt{6} \rangle| \sim n^{-\beta_{n-1}}$, and thus our scaling of λ_{n-1}, S_{n-1} might lead to some density function that is independent of n .

Matrix size n	$\langle \lambda_1 \rangle$	σ_1	Sample Size	$\frac{\langle S_i \rangle}{\sigma_{S_i}}$
				Ratios for S_1
100	4.7269	0.1060	11,000	-1.6227
200	4.8019	0.0677	11,000	-1.4344
400	4.8433	0.0419	11,000	-1.3302
500	4.8498	0.0370	9,201	-1.3288
600	4.8535	0.0354	6,000	-1.2819
800	4.8587	0.0332	6,500	-1.2139
1000	4.8615	0.0324	6,265	-1.1548
1500	4.8682	0.0306	7,348	-1.0049
2000	4.8702	0.0304	6,000	-0.9460
3000	4.8726	0.0304	6,113	-0.8584
				Ratios for S_{n-1}
100	-4.8296	0.1059	11,000	-0.6553
200	-4.8521	0.0652	11,000	-0.7193
400	-4.8681	0.0411	11,000	-0.7496
500	-4.8711	0.0363	9,201	-0.7667
600	-4.8729	0.0345	6,000	-0.7567
800	-4.8755	0.0318	6,500	-0.7380
1000	-4.8765	0.0303	6,265	-0.7412
1500	-4.8801	0.0271	7,347	-0.6987
2000	-4.8812	0.0264	6,000	-0.6710
3000	-4.8826	0.0258	6,113	-0.6337

TABLE 3.4. Empirical Ratios of $\langle S_1 \rangle$ to σ_{S_1} , and $\langle S_{n-1} \rangle$ to $\sigma_{S_{n-1}}$ for various n

4. AREAS FOR FUTURE WORK

The following are just a few possible topics for future exploration.

- *k*-Regular Random Graphs

The reason why Ramanujan graphs should consistently account for $\sim 71\%$ of our randomly generated samples of 7-regular graphs is not understood. Nor is it clear why the Tracy Widom distribution f_1 should provide a good fit to the distribution of scaled, smallest, non-trivial eigenvalues in the $k = 3$ case, but not in the $k = 7$ case. Our constructed random, 7-regular graphs are more likely to contain multiple edges than their 3-regular counterparts. Perhaps these multiple edges are affecting the distributions of S_1 and S_{n-1} . Studies of similarly generated 4-, or 5-regular, random graphs might shed light on these discrepancies. For smaller k , one could compare the edge behaviour observed in samples of simple graphs, to that observed in samples of multigraphs.

- Involutions

The adjacency matrix of a permuted toothpick graph is an involution. Studies have shown that for random involutions, the scaled length of the longest increasing subsequence is a random variable described by the Tracy-Widom distribution f_4 . Furthermore, the scaled length of the longest decreasing subsequence is described by f_1 . Is there a connection between μ_1 for a random graph of the type $A = T + P_1TP_1^{-1} + P_2TP_2^{-1} + \dots + P_nTP_n^{-1}$, and the length of the longest increasing subsequence of the the random involutions described by the matrices $P_iTP_i^{-1}$? Is there a connection between μ_{n-1} and the length of the longest decreasing subsequence? Perhaps the distributions of the longest increasing and decreasing subsequences can be used to theoretically determine the distributions of μ_1 and μ_{n-1} .

- Ihara Zeta Function

The distribution of the spacings between consecutive eigenvalues for the Gaussian unitary ensemble is known. Numerical studies have generated convincing evidence that this distribution also describes the normalized spacings of consecutive zeros of the Riemann zeta function [6]. For simple, k -regular graphs X , Ihara constructed a graph-theoretic analogue of the zeta function, $Z_X(s)$ [4]. Ihara proved that this zeta function satisfies the ‘‘Riemann Hypothesis¹’’ if and only if X is Ramanujan. It would be interesting to examine the distribution

¹All singular points of $Z_X(s)$ for which the real part of s is between 0 and 1, lie on the line $\mathbf{R}(s) = \frac{1}{2}$

of normalized spacings of consecutive zeros for this Ihara zeta function, and the distribution of scaled eigenvalue spacings for various k -regular Ramanujan graphs.

- Analysis of the Spectrum of Ramanujan Quaternion Cayley Graphs

We are currently unable to analyze the spectrum of Ramanujan quaternion Cayley graphs described in section 2.2. Because theorem 5 requires that p be greater than or equal to 5, and q be greater than p^8 , the resulting Ramanujan quaternion Cayley graphs have large vertex sets. Calculating the spectrum of the associated large adjacency matrices is computationally infeasible. As demonstrated in our example, the quaternion Cayley construction can generate Ramanujan graphs for $p < 5$ and $q < p^8$. Thus, the bounds on p and q are sufficient but not necessary for the resulting graph to be Ramanujan. For $p < 5$ or $q < p^8$, when are the quaternion Cayley graphs Ramanujan? How are the eigenvalues and eigenvalue spacings distributed?

$$\begin{array}{l}
A_{86} = \begin{bmatrix} 1 & 0 \\ 3 & 2 \end{bmatrix} \\
A_{91} = \begin{bmatrix} 1 & 1 \\ 3 & 4 \end{bmatrix} \\
A_{96} = \begin{bmatrix} 1 & 2 \\ 3 & 4 \end{bmatrix} \\
A_{101} = \begin{bmatrix} 1 & 1 \\ 4 & 0 \end{bmatrix} \\
A_{106} = \begin{bmatrix} 1 & 0 \\ 4 & 2 \end{bmatrix} \\
A_{111} = \begin{bmatrix} 1 & 1 \\ 4 & 3 \end{bmatrix} \\
A_{116} = \begin{bmatrix} 1 & 4 \\ 4 & 2 \end{bmatrix} \\
A_{87} = \begin{bmatrix} 1 & 0 \\ 3 & 3 \end{bmatrix} \\
A_{92} = \begin{bmatrix} 1 & 3 \\ 3 & 1 \end{bmatrix} \\
A_{97} = \begin{bmatrix} 1 & 3 \\ 3 & 2 \end{bmatrix} \\
A_{102} = \begin{bmatrix} 1 & 2 \\ 4 & 0 \end{bmatrix} \\
A_{107} = \begin{bmatrix} 1 & 0 \\ 4 & 3 \end{bmatrix} \\
A_{112} = \begin{bmatrix} 1 & 2 \\ 4 & 1 \end{bmatrix} \\
A_{117} = \begin{bmatrix} 1 & 3 \\ 4 & 3 \end{bmatrix} \\
A_{88} = \begin{bmatrix} 1 & 0 \\ 3 & 4 \end{bmatrix} \\
A_{93} = \begin{bmatrix} 1 & 4 \\ 3 & 1 \end{bmatrix} \\
A_{98} = \begin{bmatrix} 1 & 3 \\ 3 & 3 \end{bmatrix} \\
A_{103} = \begin{bmatrix} 1 & 3 \\ 4 & 0 \end{bmatrix} \\
A_{108} = \begin{bmatrix} 1 & 0 \\ 4 & 4 \end{bmatrix} \\
A_{113} = \begin{bmatrix} 1 & 3 \\ 4 & 1 \end{bmatrix} \\
A_{118} = \begin{bmatrix} 1 & 3 \\ 4 & 4 \end{bmatrix} \\
A_{89} = \begin{bmatrix} 1 & 1 \\ 3 & 1 \end{bmatrix} \\
A_{94} = \begin{bmatrix} 1 & 2 \\ 3 & 2 \end{bmatrix} \\
A_{99} = \begin{bmatrix} 1 & 4 \\ 3 & 3 \end{bmatrix} \\
A_{104} = \begin{bmatrix} 1 & 4 \\ 4 & 0 \end{bmatrix} \\
A_{109} = \begin{bmatrix} 1 & 1 \\ 4 & 1 \end{bmatrix} \\
A_{114} = \begin{bmatrix} 1 & 2 \\ 4 & 2 \end{bmatrix} \\
A_{119} = \begin{bmatrix} 1 & 4 \\ 4 & 3 \end{bmatrix} \\
A_{90} = \begin{bmatrix} 1 & 1 \\ 3 & 2 \end{bmatrix} \\
A_{95} = \begin{bmatrix} 1 & 2 \\ 3 & 3 \end{bmatrix} \\
A_{100} = \begin{bmatrix} 1 & 4 \\ 3 & 4 \end{bmatrix} \\
A_{105} = \begin{bmatrix} 1 & 0 \\ 4 & 1 \end{bmatrix} \\
A_{110} = \begin{bmatrix} 1 & 1 \\ 4 & 2 \end{bmatrix} \\
A_{115} = \begin{bmatrix} 1 & 2 \\ 4 & 4 \end{bmatrix} \\
A_{120} = \begin{bmatrix} 1 & 4 \\ 4 & 4 \end{bmatrix}
\end{array}$$

REFERENCES

- [1] Giuliana Davidoff, Peter Sarnak, and Alain Valette, “Elementary Number Theory, Group Theory, and Ramanujan Graphs,” Cambridge University Press, 2003.
- [2] H. Flaschka *A Random Matrix Model for the Eigenvalue Density of Regular Graphs*
- [3] B. McKay, *The Expected Eigenvalue Distribution of a Large Regular Graph* Linear Algebra Applications **40**, (1981), 203-216.
- [4] M. Ram Murty, *Ramanujan Graphs*, J. Ramanujan Math. Soc. **18**, No.1 (2003), 1-20.
- [5] Craig A. Tracy, Harold Widom *Introduction to Random Matrices* arXiv:hep-th/9210073 **v1**, (Oct 13, 1992).
- [6] Craig A. Tracy, Harold Widom *Universality of the Distribution Functions of Random Matrix Theory* arXiv:solv-int/9901003 **v1**, (Jan 6, 1999).